Modelling marine predator habitat using the abundance of its pelagic prey in the tropical southwestern Pacific

Aurore Receveur, Valerie Allain, Frederic Menard, Anne Lebourges Dhaussy, Sophie Laran, Andreas Ravache, Karen Bourgeois, Eric Vidal, Steven R Hare, Henri Weimerskirch, et al.

Modelling marine predator habitat using the abundance of their pelagic prey in the tropical southwestern Pacific

(running title: Predator habitat in the tropical southwestern Pacific)

Aurore Receveur[1,2,3,*], Valerie Allain[1], Frederic Menard[2], Anne Lebourges Dhaussy[4], Sophie Laran[5], Andreas Ravache[3], Karen Bourgeois[1,6], Eric Vidal[3], Steven R. Hare[1], Henri Weimerskirch[7], Philippe Borsa[3], Christophe Menkes[3]

[1] *OFP/FEMA, Pacific Community, 95 Promenade Roger Laroque, BP D5, 98848 Nouméa, New Caledonia.*
[2] *MIO, Aix Marseille Univ, Université de Toulon, CNRS, IRD, 13288 Marseille, France.*
[3] *ENTROPIE, UMR 250 IRD, BP A5, 98848 Nouméa, New Caledonia.*
[4] *LEMAR, IRD, Univ. Brest, CNRS, Ifremer, Campus Ifremer, BP70, Plouzané, France.*
[5] *Observatoire PELAGIS, UMS 3462, La Rochelle Université, CNRS, Pôle Analytique, 5 allée de l'Océan, 17 000 La Rochelle, France.*
[6] *IMBE, Aix-Marseille Université, CNRS, IRD, Avignon Université, Centre IRD Nouméa, BP A5, 98848 Nouméa, New Caledonia.*
[7] *Centre d'Etudes Biologiques de Chizé, UMR 7372 du CNRS-Université de La Rochelle, 79360 Villiers-en-Bois, France.*
* Corresponding author: +49 160 98703277; receveur.aurore@gmail.com

ABSTRACT

Understanding the ecological mechanisms underpinning species distribution patterns is vital in managing populations of mobile marine species. This study is a first step towards an integrated description of the habitats and spatial distributions of marine predators in the Natural Park of the Coral Sea, one of the world's largest marine protected area at about 1.3 million km², covering the entirety of New Caledonia's pelagic waters. The study aims to quantify the benefit of including a proxy for prey abundance in predator niche modelling, relative to other marine physical variables. Spatial distributions and relationships with environmental data were analysed using catch per unit of effort data for three fish species (albacore tuna, yellowfin tuna, and dolphinfish), sightings collected from aerial surveys for three cetacean guilds (Delphininae, Globicephalinae and Ziphiidae) and foraging locations identified from bio-tracking for three seabird species (wedge-tailed shearwater, Tahiti petrel and red-footed booby). Predator distributions were modelled as a function of a static covariate (bathymetry), oceanographic covariates (sea surface temperature, chlorophyll-a concentration and 20°C-isotherm depth) and an acoustically-derived micronekton preyscape covariate. While distributions were mostly linked to bathymetry for seabirds, and chlorophyll and temperature for fish and cetaceans, acoustically-derived prey abundance proxies slightly improved distribution models for all fishes and seabirds except the Tahiti petrel, but not for the cetaceans. Predicted spatial distributions showed that pelagic habitats occupied by predator fishes did not spatially overlap. Finally, predicted habitats and the use of the preyscapes in predator habitat modelling were discussed.

Key words: Micronekton, acoustic, niche modelling, Coral Sea Natural Park, cetacean, seabird, predator fish

HIGHLIGHTS
• Mapping of distribution of marine predators in one of the largest marine reserves in the world, using static, oceanographic and acoustically-derived prey covariates
• Preyscapes derived from hydro-acoustic data improves predator niche modelling
• Spatial distributions of nine predator species are mapped.

Supplementary information: See Supplementary files S1, S2 and S3 at the end of this document

INTRODUCTION

Modelling the habitat (e.g., thermal preference) of top predators is critical to understanding their spatiotemporal dynamics and developing appropriate conservation strategies. However, the way top predators are monitored largely varies among groups and can make the modelling of their habitat a challenging task. The abundance of commercially exploited species is often assessed using catch data (e.g., Lan and others 2018), and that of non-target species, using by-catch data (e.g., Escalle and others 2019) and on-board observer data (e.g., Lopez and others 2003). Non-targeted species such as cetaceans or seabirds are usually counted from boats or aircrafts. Movements of exploited and non-exploited marine predators are also monitored using a variety of tags (e.g., Block and others 2011; Abecassis and others 2015; Leroy and others 2016; Ravache and others 2020a). With some tagging methods, behaviour (foraging, migrating, resting) can be identified at various spatial-temporal scales: from a few seconds to several years, and from a few centimeters to thousands of kilometers.

Moreover, while vertical and horizontal movements of marine predators are generally assumed to be mainly motivated by foraging behaviour (Lehodey and Maury 2010), proxies of prey availability and abundance are often absent from predator niche modelling (Robinson and others 2011). Such studies are generally restricted to oceanographic (e.g., temperature, oxygen, chlorophyll-*a* concentration) and static (e.g., depth, bottom slope) variables. The absence of prey in predator niche modelling results from difficulties in quantifying their abundance and characterizing their dynamics (e.g., Escobar-Flores and others 2018; Proud and others 2018), as well as from variability in predator diet (e.g., Potier and others 2007; Olson and others 2014; Duffy and others 2015). At the local scale, predator-prey relationships have sometimes been studied using acoustically-derived prey distributions (e.g., Bertrand and others 2002a; Torres and others 2008; Lezama-Ochoa and others 2010). At the regional scale, assessments of the influence of prey distribution on predator distribution generally do not use *in situ* prey information but, rather, ecosystem model output from which preyscapes are derived (a spatial layer of prey biomass or abundance; e.g., Briand and others 2011; Lambert and others 2014; Miller and others 2018; Green and others 2020; Pérez-Jorge and others 2020). In the absence of *in situ* prey distribution observations to validate ecosystem model outputs, the reliability of such predicted preyscapes is questionable (Receveur and others 2020a).

In addition, diel vertical migration (DVM) of prey in the water column and the vertical behaviour of hunting predators influence predator-prey interactions (Schaefer and Fuller 2007, 2010; Benoit-Bird and McManus 2012; Choy and others 2017; Houssard and others 2017). Therefore, the vertical preferences and dynamics of organisms have to be taken into account in habitat predictive modelling (Opdal and others 2008; Louzao and others 2019a).

Horizontal and vertical preyscape structures around New Caledonia have been assessed using *in situ* acoustic data from at-sea surveys (Receveur and others 2019, 2020a). This region is characterized by a high richness of predators (e.g., Ceccarelli and others 2013; Laran and others 2016; Borsa and Vidal 2018), which issupported by a diversity of prey (Allain and others 2012; Williams and others 2015; Receveur and others 2020b). This high diversity motivated the creation of the Natural Park of the Coral Sea covering the entire New Caledonia exclusive economic zone (EEZ, 1.3 million km²; Martin and Lecren 2014). The creation of this large Natural Park has emphasized the need for robust scientific information on the pelagic ecosystem status and potential anthropogenic threats (Ceccarelli and others 2013; Gardes and others 2014). In the present study, a statistical model combining environmental covariates and vertically-structured prey abundance with top predator abundance and occurrence data, was developed for New Caledonian waters. The benefit of including a proxy for prey abundance (the acoustic echo intensity integrated over different depth layers) in predator niche modelling, in addition to that of other marine physical variables, was quantified. Statistical relationships were then used to predict and map the spatial distributions of the nine selected marine predators.

METHODS

Statistical models were fitted to indices of predator abundance and occurrence as a function of covariates that included prey distribution and other biotic and abiotic oceanographic conditions. Our domain of investigation covered the New Caledonia EEZ (14°S–27°S, 156°E–175°E, Figure 1).

Covariates

Five biophysical oceanographic variables and a proxy for biotic prey comprised the six environmental variables used to explore drivers of predator abundance/occurrence (Supplementary Table S1). All covariates were extracted or predicted at the date and position of each predator observation. Bathymetry was extracted from the ZoNéCo database at a 500-m spatial resolution (ZoNéCo, 2013). Sea-surface temperature (SST) was extracted from the NOAA OI SST high resolution dataset (Reynolds and others 2007). The depth of the 20°C isotherm was extracted from the Armor3D dataset (Guinehut and others 2012). Surface chlorophyll-*a* concentration was extracted from GLOBCOLOUR (Saulquin and others 2011). SST, depth of the 20°C isotherm and chlorophyll-*a* concentration were extracted on a ¼ degree spatial grid, with a weekly temporal resolution.

Prey data

The preyscapes were derived from the 3-D statistical model developed by Receveur and others (2019), which relates micronekton vertical distribution obtained from acoustic data to environmental conditions in the Coral Sea region. Acoustic data collection, statistical methodology, and validation of micronekton biomass estimates in the New Caledonia EEZ are detailed in Receveur and others (2019) and in Supplement 2. Acoustic data, covering more than 17,500 km of line transect, were collected during six cruises from 2011 to 2017 (Supplementary Figure S3 and Table S3; Allain and Menkes 2011), using an EK60 echo sounder (SIMRAD Kongsberg Maritime AS, Horten, Norway). After processing, 38 kHz acoustic data were echo-integrated to provide the nautical-area scattering coefficient (NASC, in $m^2.nmi^{-2}$), a proxy for micronekton biomass (Maclennan and others 2002; Irigoien and others 2014; Proud and others 2017). It is important, however, to keep in mind that gas-filled organisms (e.g., fishes with a swim bladder) are largely dominant in the NASC38 kHz signal, while other organisms without gas are poorly represented (Davison and others 2015).

   The final dataset was then composed of 16,715 acoustic vertical profiles deployed between 10 m and 600 m, excluding transition periods at dawn and dusk. A machine-learning model (XGBoost, a machine learning regression tree) was fitted to link the acoustic vertical profiles to environmental explanatory variables: norm of the wind, 0-600 m mean temperature, 0-600 m mean oxygen, 0-600 m mean salinity, surface chlorophyll, bathymetry and sun inclination (Supplementary Figure S4, left column). This model enabled us to robustly predict (with a success rate of 87% of in cross validation and Supplementary Figure S5) a proxy for the vertical micronekton biomass (NASC profiles) for the entire New Caledonia EEZ.

   NASC profiles were predicted on a regular ¼° spatial grid and ona weekly temporal resolution (Supplementary Figure S4, right column) for day and night periods. Predicted NASC profiles were then integrated to obtain the day and night preyscapes over four vertical layers that were defined according to predators' behaviour (see "Statistical analysis for niche modelling" section): 10-30 m (sub-surface; 'sub_surf'), 10-200 m (*i.e.* epipelagic layer; 'epi'), 200-400 m (*i.e.* upper mesopelagic layer; 'up_meso') and 400-600 m (*i.e.* lower mesopelagic layer; 'low_meso') (Figure 2).

Predator data collection

Tuna and dolphinfish

Predator fish abundance was inferred from fishery daily catch rates (Table 1, Figure 3). Daily catch rates (number of fish per hundred hooks) of albacore tuna (*Thunnus alalunga*, ALB), yellowfin tuna (*Thunnus albacares*, YFT) and dolphinfish (*Coryphaena hippurus*, DOL) were obtained from the logbooks of all longliners operating in the New Caledonian EEZ from 2010 to 2018 (Anonymous 2018). The logbooks provided information on a daily basis: name of vessel, date and location (latitude and longitude) of the beginning of the fishing set, number of hooks, and number of specimens captured per species. The logbook data from the New Caledonia fishing fleet are considered highly reliable; 100% of logbooks are received by the Direction des affaires maritimes, fishing locations recorded in logbooks are verified against vessel monitoring system data for each set, while catch species and quantities are verified by on-board fisheries observers and port samplers.

Cetaceans

Cetacean counts were obtained from a large-scale aerial survey of the New Caledonia EEZ made between October and December 2014 (REMMOA survey: Laran and others 2016a; Table 1). More than 30,000 km line transect were surveyed over a total surface area of 542,300 km^2 (39% of the EEZ, Figure 3) at a ground speed of 90 knots and an altitude of 600 feet. A line-transect methodology was used to count cetaceans (Buckland and others 2001) from high-wing double engine aircrafts equipped with bubble windows enabling vertical observation of the sea surface. Cetacean group size was recorded at the lowest possible taxonomic level, alongside observation conditions (Beaufort Sea-state, glare severity, turbidity, subjective condition and cloud coverage). Cetacean observations were summed over 10-km segments of effort with homogenous weather conditions. Only segments with good weather conditions (i.e., Beaufort sea state ≤ 3 and subjective condition medium, good or excellent) were kept. Perpendicular distances from the track line were obtained from clinometer measurements by observers.

As the number of observations per species was relatively small, we grouped species into energetic guilds based on morphological features and diving capabilities (Lambert and others 2014; Mannocci and others 2014a, 2014b). These authors considered diving ability as a proxy for energetic requirements to classify tropical odontocete species into three guilds: Delphininae (DELPH), Globicephalinae (GLOB) and Ziphiidae (ZIPH). The DELPH guild was composed of small Delphininae [*Stenella longirostris* (9% of sightings), *S. attenuata* (9%) and unidentified *Stenella* spp.] and large Delphininae including *Tursiops truncatus* (21%), *T. aduncus* (19%), *Lagenodelphis hosei* (7%), and unidentified large Delphininae. The GLOB guild was composed of *Globicephala macrorhynchus* (52%), *Grampus griseus* (16%), *Pseudorca crassidens* (8%), *Peponocephala electra* (3%) and unidentified small and large Globicephalinae (3% and 16%, respectively). The ZIPH guild included *Ziphius cavirostris* (41%), *Indopacetus pacificus* (18%), *Mesoplodon* spp. (20%), and possibly other, unidentified beaked whale species.

Seabirds

Seabird positions were obtained from GPS-tracking surveys in 2012 and 2015 (in May, June and November) for the red-footed booby (*Sula sula*, RFBO; 21 individuals equipped), and in 2017, 2018 and 2019 (in January, June, and from August to December) for the Tahiti petrel (*Pseudobulweria rostrata*, TAPET; 21 individuals equipped), both present year-round in New Caledonian waters (Table 1; Borsa and others 2010). The wedge-tailed shearwater (*Ardenna pacifica*, WTSH; 68 individuals equipped), present in the area during the breeding season only, i.e. between October and May (Weimerskirch and others 2020), was tracked in 2017, 2018 and 2019 (in March and April).

GPS receivers were attached to adult WTSH during the chick-rearing period at five study colonies (Supplementary Figure S2). The Pindaï study colony is located on New Caledonia's main island [colony size (*N*) = 11,000 breeding pairs; see Supplementary Table S2 for detailed references]. Three other study colonies (Tiam'bouene, *N* = 11,520; Canards, *N* = 340; and Mato, *N* = 2000) were lagoon islets, located

less than 20 km from the main island. The farthest study colony was Loop islet in the Chesterfield atoll (*N* = 11,000), located 600 km NW of New Caledonia's main island. Details concerning the deployment of the GPS receivers have been presented previously (Ravache and others 2020a; Weimerskirch and others 2020).

GPS-tracked TAPET were from the Mato (*N* > 20 breeding pairs) and Nemou (diffuse colony of a few hundred breeding pairs) study colonies, the latter being located in the eastern lagoon of New Caledonia (Ravache and others 2020b).

GPS-tracking experiments on adult RFBO were conducted on colonies from the Chesterfield atoll (*N* = 3540) in 2012 and Surprise islet (*N* = 2883) (Entrecasteaux atoll, 200 km north to New Caledonia's main island) in 2015 (Mendez and others 2017, 2020).

The geographic distribution of the WTSH and TAPET study colonies was deemed representative of the populations of these two species across the New Caledonian EEZ (see Supplementary Table S2). The two RFBO colonies sampled were among the largest within the New Caledonian EEZ and were located in its northern half; two other major colonies located in the south eastern part of the New Caledonian EEZ (Walpole and Hunter; Supplementary Table S2) were not sampled.

The expectation-maximization binary clustering (EMbC) algorithm (Garriga and others 2016) was used to classify seabird movements in four behaviourial categories. EMbC is a robust multivariate clustering algorithm based on trajectory sinuosity and speed, allowing identification of specific behaviours. It assumes that wide turning angles between consecutive locations indicate foraging behaviour, while fast and straight bouts are associated with commuting movement. One of the four following behaviours was assigned to each GPS position using the EMbC method: resting (low speed, small turning angle), commuting (high speed, small turning angle), extensive search (high speed, wide turning angle) or intensive foraging (low speed, wide turning angle). Movement bouts including at least three consecutive 'intensive foraging' locations (and 'intensive foraging' or 'extensive search' for TAPET, Ravache and others 2020b) were then conserved as 'foraging presence' locations, while the other locations were considered as 'foraging absence' locations for further analysis.

Statistical analysis for niche modelling

Generalized additive models (GAMs; Hastie and Tibshirani 1990) and generalized additive mixed models (GAMMs) were used to examine relationships between predator abundance/occurrence (the response variable) and a suite of covariates (i.e., bathymetry, SST, chlorophyll-*a* concentration, d20 and NASC, Table S1). Absence of collinearity between pairs of covariates was tested using Spearman's rank correlation test (below 0.5, Louzao and others 2011). All variables were smoothed with cubic splines with a maximum knot number set to eight for tunas and four for the seabirds and cetaceans due to the limited number of data, to prevent overfitting. Residual checks were conducted for the nine models using quantiles (Dunn and Smyth 1996) : residual variance was constant, residuals were independent, and neither predicted values and residuals nor explanatory variables and residuals were statistically linked.

Models were fitted successively, excluding each of the remaining terms one at a time, to assess the percentage of variation explained by a predictor and to classify predictors according to the magnitude of their influence in the model.

Models for tunas and dolphinfish

For fishes, the response variable of the three GAMs was the number of specimens caught. The logarithm of the number of hooks was added as an offset to consider the variability in fishing effort among trips. A random effect by vessel was also fitted to deal with the variability in catchability among vessels. Year was added as a continuous explanatory variable to assess possible temporal change, and spatial smoothing in latitude and longitude was added to account for spatial autocorrelation (Table 2).

As the exact time of the catch by commercial longliners was unknown, NASC values integrated by depth class were averaged over day and night. Only the epipelagic layer was considered for DOL (Furukawa and others 2014; Lin and others 2019); the epipelagic and the upper mesopelagic layers were chosen for YFT (Dagorn and others 2006; Schaefer and others 2009); while the epipelagic, and the upper and lower mesopelagic layers were used for ALB (Williams and others 2015).

Models for cetaceans

For cetaceans, the response variable of the three GAMs was the number of individuals counted along the flight track per approximately 10-km long segment. To estimate the sample area, effective strip width was used (ESW), estimated as the point at which the number of schools detected beyond is equal to the number of schools that are missed within (Marques and Buckland 2004). The area sampled for each single segment was the length multiplied by twice the corresponding associated ESW. The log-transformed sampled area was added as an offset in the model to account for the variability in sampling effort. ESW for these data sets were estimated by Laran and others (2016a).

As aerial surveys were conducted during the day, NASC values were used for the day period only, and included the epipelagic, upper and lower mesopelagic layers (Lambert and others 2014).

Models for seabirds

For seabirds, GAMMs were used to account for autocorrelation between consecutive behaviours in an individual. An autocorrelation structure of order two with a random effect fitted by individual was nested to deal with the correlation structure (Wood 2006; Dormann and others 2007). The response variable of the three GAMMs was the occurrence of foraging behaviour.

Using the GPS time stamp, we calculated sun inclination (Michalsky 1988; Blanc and Wald 2012) to estimate the period of the day (negative sun inclination values for night and positive values for day) of each spatial location. NASC values were then used for the corresponding moment of the day (day or night), and the sub-surface layer (10-30 m) was used, i.e., the vertical layer used by these species to forage (Table 2). The first 10 meters were missing as they are not recorded by the echosounder and therefore not present in the acoustic modelling (Receveur and others 2019).

Prediction protocol

To avoid predictive extrapolation, predictions were limited to sampled environmental variable ranges hence the presence of blank areas in the prediction maps, particularly visible for seabirds. Moreover, to avoid temporal extrapolation, predictions were made only for months when data were collected (given in Table 1).

The predictions were made on a regular 0.25-degree spatial grid based on environmental and NASC values, on a weekly temporal resolution, for all weeks of surveyed months between 2010 and 2019. For visualization, the predictions were then averaged over three month periods (DJF: December, January and February; MAM: March, April and May; JJA: June, July and August; SON: September, October and November) over the 2010-2019 period. For the NASC values, the same vertical layers and night/day periods (i.e., night-day mean for fish, day for cetaceans and night and day separated for seabirds) were used as for the fitted models (Table 2). As the fine-scale robust bathymetry used was available only for the New Caledonian EEZ (ZoNéCo 2013), predictions were limited to this EEZ.

The three fish models were used to predict catch values with an offset of number of hooks set to the mean value over the studied years (1960 hooks/longline set). To obtain catch per unit of effort (CPUE), a proxy for fish abundance, predicted catches in each grid cell were divided by the offset.

For cetaceans, the number of individuals was predicted with an offset of sampled area set to a mean value (4 km²). To obtain density of individuals (no./km²), predicted numbers of individuals in each grid cell were then divided by the offset.

Finally, for the three seabird species, the model directly predicted the probability of occurrence of foraging behaviour. The breeding parents are spatially limited to the region they can reach by their flying ability and by the time that they can spend away from their chick. Therefore, the maximal distance travelled from the colony was calculated based on the datasets for each species (774 km for WTSH, 1079 km for TAPET, and 320 km for RFBO), and the predictions were spatially limited to the circle with a radius equal to this maximal distance. For WTSH and TAPET, the predictions were limited by this maximal distance around the sampled colonies. For the RFBO, three well-known colonies were added in the south of the EEZ (Supplementary Figure S2), and the predictions were limited around these five (two sampled and three well-known) colonies.

All analyses were conducted using R version 3.5.0 (R Core Team 2016) and GAMs were done using the *mgcv* package (Wood 2017). The R script used for modelling and predictions is given in Supplement 3.

RESULTS

Environmental and prey layers

Bathymetry is complex in the New Caledonia EEZ (Figure 1A), with deep waters in the north and the southeast (~ 5 km), shallower waters in the southwestern corner and south of the main island (~ 3 km), and the deep New Hebrides trench in the east (>7 km deep; Stewart and Jamieson 2018).

On average, for the 2010-2019 period, relatively warmer SSTs occurred in the north (~ 24°C) and colder SSTs in the south (~ 18°C) (Figure 1B). Mean depth of the 20°C-isotherm was about 160 m in the south and about 210 m in the north with the deepest values (~ 230 m) located west of the Chesterfield reefs (Figure 1C). Chlorophyll-a concentration was high close to coasts and reefs, and generally higher in the south of the main island compared to the north.

As for SST and the 20°C-isotherm depth, NASC spatial distribution showed a strong latitudinal gradient, especially during the night, with values in the south almost twice as high as values in the north on average for the 2010-2019 period (Figure 2). During the day, between 0 and 30 m, the largest NASC values were close to the coast of the main island and in the south. The 200-400 m integrated NASC showed similar spatial patterns. The 0-200 m and 400-600 m integrated NASC were higher in the south than in north.

Predator data

ALB, YFT and DOL datasets were composed of 14,941, 17,420 and 17,106 longline sets, respectively, collected between January 2010 and December 2018. The number of fish caught per 100 hooks, calculated by set, ranged between 1 and 26.5 (ALB), 1 and 9.1 (YFT) and 1 and 3.3 (DOL). The EEZ was fished across its entirety, except for small regions in the southeastern corner and in the extreme north (Figure 3).

Cetacean data were distributed more sparsely, with spatial and temporal observation coverage lower than for fish. There were around 2,500 segments, but with a low number of sighting occurrences (between 31 and 40 according to the cetacean guild). The encounter rates (number of individuals per sampled km²) ranged from 0 to 26.7 for DELPH, from 0 to 163.8 for GLOB (with only two rates larger than 10), and from 0 to 1.5 for ZIPH (Figure 3).

For seabirds, temporal sampling effort was limited by the breeding season, when animals were present in New Caledonia (Table 1). The number of recorded GPS positions varied substantially among species, with more than 11,500 observations for WTSH (including 3934 eating occurrences), more than 6,500 for

RFBO (including 1547 eating occurrences), and more than 4500 for TAPET (including 1586 eating occurrences).

Environmental drivers of predator distribution

Importance of prey distribution

Total deviance explained by abundance/occurrence models ranged from 7.3% (DELPH) to 31.7% (GLOB) (Table 3). The NASC variable had a relatively small influence in all models, although it ranked second for WTSH and RFBO, third in YFT, fourth in DOL and fifth in ALB (Table 3). Relationships to NASC were weak and non-significant for DELPH, GLOB, ZIPH and TAPET (Figure 4) with very low deviance explained by these variables (Table 3).

   ALB abundance was positively linked to NASC values in the epipelagic and lower mesopelagic layers: the higher the NASC values, the larger the predicted CPUE (Figure 4), and negatively linked in the upper mesopelagic. DOL abundance was positively linked to epipelagic NASC values. YFT relationships with epipelagic and upper mesopelagic NASC were negative, with a steeper slope for the epipelagic than for the upper mesopelagic NASC. For ALB and DOL, NASC influence was relatively small compared to the total deviance explained while it was five times higher for YFT (Table 3).

   WTSH foraging probability was linearly positively related to 10-30 m NASC values during the day, while the relationship exhibited a bell shape during the night (Figure 4). The NASC variable was the second most important driver of this species' foraging probability as it explained 6.7% of the deviance (Table 4). RFBO foraging probability was negatively linked to NASC values during the day (Figure 4) and NASC relative importance in RFBO model ranked second with 5.7% explained deviance (Table 4). The flat relationship between NASC and TAPET foraging probability demonstrated the non-significance of the relationship (Figure 4).

Other oceanographic drivers

For the predatory fishes, the four other environmental covariates were almost all statistically significant but their influence ranked differently across species (Table 3). YFT and DOL CPUEs were most influenced by chlorophyll-*a* concentration and ALB CPUE by SST. Bathymetry was the second influencing factor for ALB and YFT, and SST ranked second for DOL.

   Optimal environmental values varied among fish species (Figure 5): higher ALB catch was predicted for intermediate bathymetry (around 4 km), whereas YFT catch was highest for shallower bathymetry (shallower than 2 km), and DOL catch was highest for bathymetry deeper than 4 km depth. Maximum YFT catch was predicted for intermediate chlorophyll values (0.2-0.4 mg.m^{-3}), whereas DOL catch was highest for low chlorophyll-*a* concentration values (below 0.1 mg.m^{-3}). The relationship with chlorophyll for ALB was almost flat. Colder SST (below 22.5°C) was favourable to ALB catch whereas warm SST increased YFT and DOL catch (about above 27°C). ALB and DOL catch increased with 20°C-isotherm depths greater than 200 m depth; conversely, YFT catch was higher when the 20°C-isotherm was shallower than 200 m depth (Figure 5).

DELPH abundance was mostly influenced by chlorophyll-*a* concentration; GLOB abundance by the 20°C-isotherm depth; and ZIPH abundance, by chlorophyll-*a* concentration (Table 3). Higher DELPH abundance was predicted in waters with low chlorophyll-*a* concentration (below 0.1mg.m^{-3}) and cold SST (< 25 °C). GLOB abundance was predicted to be higher when the 20°C-isotherm was deep, when the depth was either shallower than 2 km or deeper than 4km, and in waters with low chlorophyll-*a* concentration. ZIPH abundance was predicted to be higher in waters with intermediate chlorophyll-*a* concentrations (about 0.8 mg.m^{-3}), around 3 km deep, with warm SST and with a 20°C-isotherm depth at around 150 m (Figure 5).

Foraging behaviour of the three seabird species was primarily influenced by bathymetry, but with contrasting optimal values: WTSH mostly fed where waters were deeper than 2 km while TAPET and RFBO fed in waters shallower than 2 km (Figure 5). Secondarily, WTSH foraging behaviour was positively influenced by high NASC values (above 5m^2.nmi^{-2}) integrated between 10 and 30 m deep, and when 20°C-isotherm depth was shallower than 150 m. TAPET was predicted to more likely feed in waters with chlorophyll-*a* concentration > 0.2 mg.m^{-3}. RFBO foraging behaviour was also influenced by SST, with more feeding predicted to occur in warm waters in general.

Spatial distribution predictions

Predator spatial distribution

The preferred habitats for ALB, YFT and DOL, indicated by predictions of high CPUE, did not spatially overlap (Figure 6). Higher ALB CPUE was generally predicted west of New Caledonia's main island. The largest CPUE was predicted west of the Chesterfield reef, except for a small area of low CPUE directly surrounding the Chesterfield and Bellona atolls (reef and island names are indicated on Figure 1A). Conversely, high predicted YFT CPUE was predicted in this small area. Higher YFT CPUE was predicted close to the lagoon, around the main island, especially in the north, around the d'Entrecasteaux atolls, and to a lesser extent around the Loyalty Islands. Finally, the channel between the main island and the Loyalty Islands was predicted to be the most favorable for high DOL CPUE. Predicted standard errors were larger in the southeast of the New Caledonia EEZ, and lower than 10% for the rest of the EEZ (Figure S6).

Higher DELPH abundance in the EEZ was predicted to the southeast and south of the main island between September and November, while a hotspot was predicted for this cetacean guild in the northern part of the EEZ between December and February (Figure 7). GLOB were predicted to occur most frequently in the extreme north of the EEZ and around the Lansdowne bank. ZIPH were predicted to occur around Chesterfield reefs and between the main island and the Loyalty Islands between September and November, and especially between the main island and the Loyalty Islands between December and February. For the three cetacean guilds, predicted standard errors were high, on average larger than 50% for DELPH and GLOB, certainly linked to the (low) performances of the models (Supplementary Figure S7).

WTSH were predicted to feed mostly north of 19°S when the species is present in New Caledonian waters. TAPET mostly fed in waters south of the main island in shallow waters (close to the lagoon), south of Bellona and above the Lansdowne bank, between Chesterfield and the main island (Figure 8). Predicted standard errors for WTSH and TAPET were below 20% (Supplementary Figure S8). No clear foraging hotspot was identified for RFBO: predictions showed scattered areas around the EEZ mid-latitudes, always close to the two studied colonies; but predicted standard errors were higher than 60% during the period extending from June to November.

DISCUSSION

Previous studies on marine predators in the tropical southwestern Pacific have focused on specific predator groups including seabirds (Pandolfi-Benoit and Bretagnolle 2002; Borsa and others 2010; McDuie and others 2015; Mendez and others 2017, 2020; Ravache and others 2020a,b; Weimerskirch and others 2020), cetaceans (Garrigue and others 2015; Laran and others 2016; Derville and others 2019, 2020), sharks (Tirard and others 2010; Boussarie and others 2018) and albacore tuna (Briand and others 2011; Williams and others 2015) in separate publications. This study represents the first attempt to reach an integrated, quantitative, multispecies view of marine predator trophic ecology across the Coral Sea pelagic ecosystem. Prey abundance as estimated through acoustic surveys was tested together with oceanographic covariates to improve predator distribution models. Preyscape significantly affected five predator distribution

patterns out of nine, but their influence remained small relative to other predictors and they did not rank as the most important variable for any species.

Sources of uncertainty linked to predator data

Fishing vessels in New Caledonia are longliners with similar fishing capabilities (Anonymous 2018). By including a random 'vessel' effect, we considered the potential variability of fishing power between vessels. By including the effort (i.e., number of hooks) as an offset, we transformed catches into CPUE, which was then used as a proxy for fish abundance. Although large differences in CPUE can be erroneously measured where only small differences in abundance exist (Kleiber and Maunder 2008), our modelling approach incorporating a large dataset of fishing operations is likely a reliable proxy for fish abundance.

Compared to CPUE data, the three-month aerial survey REMMOA, which only occurred once in New Caledonian waters, only gives a snapshot of animal presence and partial distribution over a short period. Cetaceans are highly mobile predators; they may have been travelling between favorable habitats when spotted and therefore the oceanographic conditions attributed to that group were not necessarily optimal foraging habitats. Furthermore, aerial surveys cannot detect the presence of animals when they are diving, which then represent false absence values in the model. Improving our niche modelling of cetacean habitats may require additional aerial survey effort to better characterize their distribution.

For seabirds, uncertainty was linked to the clustering algorithm that identified behaviour based on trajectory sinuosity and speed. Here, by selecting only the intensive foraging observations occurring for more than three consecutive positions, we ensured that the animals were robustly classified as foraging.

In the present study, we mostly selected adult individuals for fish (through catch) and seabirds (through GPS-tracking). For future studies, it would be important to include juvenile, immature and non-breeding animals which represent a significant part of a population. Immatures and non-breeders may use habitats different from breeding adults (Mendez and others 2016, 2020; Houssard and others 2017; Weimerskirch and others 2020). However, this objective would require the use of different sampling techniques and the development of modelling strategies mixing different sampling methods (e.g., aerial count for seabirds together with tracking methods) for one species.

Acoustic-micronekton layers for predator niche modelling

Our approach relied on a large dataset to robustly predict preyscape at a large spatial-temporal scale. For a given observed acoustic value, the predicted acoustic value varied by ± 10dB (Receveur and others 2019; Supplementary Figure S5), which could result in large biomass changes (Benoit-Bird 2009; Proud and others 2019). However, predicted acoustic spatial and temporal variations matched observed variations (see figure 11 of Receveur and others, 2019).

The use of the 38 kHz frequency favoured the detection of organisms with gas-filled organs (e.g., fishes with a swimbladder) while excluding organisms without gas (Davison and others 2015), which may bias our perception of the spatial variation of prey abundance (Proud and others 2019, 2018). Nevertheless, given the large diversity in predator diet (Olson and others 2014; Duffy and others 2015; Williams and others 2015) and the difficulty in transforming acoustic signal into species-specific biomass (Davison and others 2015; Proud and others 2019), we used NASC values as a proxy for the relative abundance of prey available to all predators. Separating the acoustic signal into species groups (such as 'fish', 'gelatinous', or 'crustacean') would allow linking each predator to its favorite prey. We assumed that a large part of the weakness of the trophic relationships was linked to this acoustic value, which does not fully represent the specific diet of each predator.

Another acoustic limitation was linked to the fine horizontal scale (e.g., prey aggregations in shoal) that was removed from the acoustic signal in the statistical framework, although it is an important component of foraging behaviour (Benoit-Bird and Au 2003; Bertrand and others 2014; Grados and others 2016).

More positively, one strength of our acoustic modelling framework was its ability to average relative prey abundance over different vertical layers. Prey layers were defined according to the predators' vertical feeding habitats as reported from the literature. The differences in spatial patterns during the day of integrated NASC values over depth layers 10-30 m and 10-200 m (Figure 3) confirmed the relevance of extracting specific vertical layers to analyze prey-predator relationships. Integrating the vertical dimension is a necessity to define the 3-D oceanographic habitats used by marine species (Lambert and others 2014; Brodie and others 2018; Louzao and others 2019a).

In previous studies, two approaches were used to implement prey abundance in predator niche modelling: (1) by simultaneously collecting prey data and observing megafauna (e.g., Doray and others 2018; Louzao and others 2019b; Putra and Mustika 2020); and (2) by using SEAPODYM, an end-to-end ecosystem model (Lehodey and others 2008, 2010) prey output (Briand and others 2011; Lambert and others 2014; Miller and others 2018; Green and others 2020). Our study suggests a third alternative where prey abundance is estimated during previous acoustic surveys focusing on low trophic levels, with limitations detailed above, and then compared to predator observations from other surveys. Such an approach could be useful for predator sampling techniques with which it is impossible to collect prey data at the same time (e.g., aerial survey and telemetry). Our approach enabled us to study predator-prey relationships at the regional scale based on *in situ* prey data, but required acoustic observations at this vast spatial scale. The use of a machine-learning algorithm to extrapolate the acoustic signal to the whole EEZ helped make robust predictions, with a success rate of 87% in cross validation. Receveur and others (2021) validated for the Coral Sea region the extrapolation of acoustic signal in the epipelagic layer by comparing it to the outputs of an ecosystemic model (SEAPODYM). Conducting more acoustic surveys through e.g. routine acquisition by commercial ships, and improving the relationships between acoustic signal and species composition and biomass, would help refine prey distribution models which, in turn, would improve prey implementation into predator niche models.

Predators habitat

Tunas and dolphinfish were strongly influenced by SST: YFT and DOL preferred warm SST, whereas the optimal SSTs for ALB were colder (Bertrand and others 2002b; Kleisner and others 2010; present results). ALB's relationships to NASC values were in agreement with previous results found in the New Caledonia EEZ using the SEAPODYM outputs as prey data source (Briand and others 2011). Briand and others (2011) showed a positive relationship between ALB CPUE and epipelagic layer prey biomass and found a negative relationship to upper mesopelagic prey biomass, similar to our results (Figure 4).

To explain the negative relationship to upper mesopelagic prey, these authors assumed that the increase in prey abundance induced a competition for baited hooks located in the mesopelagic layer. This hypothesis was confirmed by a study on albacore tuna in French Polynesia (Bertrand and others 2002b). This hypothesis would also explain the negative relationships of YFT catch values to NASC values. ALB, YFT and DOL exploit comparable foraging resources and have similar niches (Teffer and others 2015), especially YFT and DOL in the Pacific (Young and others 2010). Here, we instead observed a relatively weak distributional overlap between the three species (except for DOL and YFT east of the New Caledonian main island, Figure 6A) and different relationships to environmental predictors. We hypothesize that the data obtained at the scale of the Pacific Ocean for ALB, YFT and DOL show roughly similar distributions but that at a smaller scale, the spatial distributions of the three species can be distinguished based on their habitats. For instance, Bertrand and others (2002) showed that tunas were more abundant in waters rich in prey and with favorable hydrological conditions at a regional scale (e.g., Polynesian EEZ scale), and were attracted by small prey patches at smaller scale in the southeast Pacific. We confirmed this result here for ALB, but found that YFT was more abundant in waters with relatively low prey abundance. The 20°C-isotherm depth was relatively important to explain the presence of the two tuna species. It is a proxy for vertical habitat change but it is strongly linked to catchability changes.

Therefore, part of the abundance changes linked to the 20°C-isotherm depth may also reflect catchability changes rather than a true ecological relationship.

Chlorophyll-a concentration and the 20°C-isotherm depth (GLOB and ZIPH), together with SST (DELPH) influenced the distribution of the cetacean predators in New Caledonia, as previously shown elsewhere in a tropical region (Mannocci and others 2014a). The three bell-shaped relationships with the chlorophyll-a concentration identified here, were in agreement with previous published work in the circumtropical belt (Mannocci and others 2015). This study also emphasized the non-negligible influence of the depth of the minimum dissolved oxygen concentration, a variable that we did not include. The absence of this parameter may explain the relatively low model performances of the three cetacean guilds of the present study. The positive linear relationship between ZIPH abundance and SST was also already demonstrated in the South Pacific gyre (Mannocci and others 2014a). NASC values were non-significant for the three guilds in our study. This must be linked to the acoustic signal. Indeed, as discussed in the "Acoustic-micronekton layers for predator niche modelling" section, the acoustic signal encompasses a large variety of micronekton species dominated by gas-filled organisms. However, cetacean diet species are likely poorly represented in the acoustic signal, explaining the absence of a significant relationship. The SEAPODYM micronekton model includes these cetacean diet species, as Lambert and others (2014) found significant trophic relationships for cetacean; thus that may be a more suitable approach to study cetacean trophic relationships. Lambert and others (2014) also noted that delphinids mostly forage at night. The use of day-only NASC values in our modelling may also limit the strength of the fitted relationships.

Finally, cetacean species were grouped based on morphological and taxonomic characteristics, to delimit energetic guilds, while other taxonomic groups were studied at the species level. This grouping leads to a mix of different habitats while adjusting a single habitat model, which might have contributed to the low explained deviances. However, these guilds also correspond to energetic considerations and, therefore, the grouped species have a similar habitat. In addition, this strategy is needed to increase the robustness of the model considering the low number of sightings by species. Finally, this approach allowed the full exploitation of aerial survey data in which identification to the species level was not always possible.

Seabird relationships to oceanographic conditions were in agreement with previous results in the western Coral Sea (McDuie and others 2018). Among the variables tested, bathymetry had the strongest influence on all three species, as already demonstrated for WTSH in the Indian Ocean (Catry and others 2009). Relationships to the 20°C-isotherm depth were mostly negative for WTSH and RFBO. Such relationships may reflect the fact that at a large scale, shallower 20°C isotherms characterize regions with usually higher primary production. Moreover, the 20°C-isotherm depth is linked to the position of meso-scale eddies, which have been shown to influence foraging behaviour of seabirds (Tew Kai and others 2009; Tew Kai and Marsac 2010; Jaquemet and others 2014; McDuie and others 2018). Indeed, meso-scale eddies potentially structure vertical and horizontal prey abundance, with large variability of demonstrated effects (Sabarros and others 2009; Godo and others 2012; Della Penna and Gaube 2020). More detailed spatial data and localization of eddies would be required to understand these relationships. The difference in NASC relationships between day and night in WTSH suggested that WTSH can locate prey concentration near the surface during the day, whereas other feeding techniques might be used during the night. This confirmed the results of Ravache and others (2020a), who found that WTSH feeding behaviour was higher during the full-moon nights due to higher luminosity. TAPET did not target areas with high prey abundance but foraged over shallow waters with high chlorophyll-a concentrations. The absence of a relationship to NASC values confirms results showing that TAPET have a scavenging foraging behaviour and mostly target isolated prey (Ravache and others 2020b). For the RFBO, the radius of the prospective habitat reached is smaller than for the two other seabirds species (Mendez and others 2017, 2020; Ravache and others 2020b; Weimerskirch and others 2020; present results). This can explain the large confidence interval predicted around the NASC relationship: the RFBO individuals found their food at proximity and are not able to prospect on larger scale to target high prey concentration.

CONCLUSION

We developed a niche modelling approach to evaluate the role of environmental predictors, including preyscape and other oceanographic conditions, to characterize the spatial distribution of nine marine predators in the south-west Pacific region. The inclusion of the different preyscapes based on *in situ* data was especially innovative and interesting. Our approach illuminated different trophic interactions and behaviours (e.g., different across the species considered, different across the vertical layers, different between day and night). To further develop this approach, a variety of additional taxa (e.g., sea turtles, sharks) could be added and would provide a more exhaustive overview of predator-prey relationships in the pelagic ecosystem.

DATA AVAILABILITY

The different data used in the study are available upon request. Acoustic data (EK60 recording) can be requested from receveur.aurore@gmail.com; christophe.menkes@ird.fr; and anne.lebourges.dhaussy@ird.fr. Raw fish data (longline logbook) are protected data; valeriea@spc.int and stevenh@spc.int can be contacted to inform about the formalities. Cetacean data (count) are accessible from the PELAGIS Observatory data set page of OBIS (https://obis.org/dataset/2101d4c5-c20b-49c0-a44b-3d6484c4c891) or can be requested from sophie.laran@univ-lr.fr. Seabird data (GPS tracking) may be available upon request from eric.vidal@ird.fr; henri.weimerskirch@cebc.cnrs.fr, andreas.ravache@ird.fr, and karen.bourgeois2@gmail.com (wedge-tailed shearwater and Tahiti petrel); and henri.weimerskirch@cebc.cnrs.fr and philippe.borsa@ird.fr (red-footed booby).

REFERENCES

Abecassis M, Polovina J, Baird RW, Copeland A, Drazen JC, Domokos R, Oleson E, Jia Y, Schorr GS, Webster DL, Andrews RD. 2015. Characterizing a foraging hotspot for short-finned pilot whales and Blainville's beaked whales located off the west side of Hawai'i Island by using tagging and oceanographic data. PLoS One 10:e0142628.

Allain V, Fernandez E, Hoyle SD, Caillot S, Jurado-Molina J, Andréfouët S, Nicol SJ. 2012. Interaction between coastal and oceanic ecosystems of the western and central Pacific ocean through predator-prey relationship studies. PLoS One 7:e36701.

Allain V, Menkes C. 2011. Nectalis 1-5 cruises. RV Alis. https://campagnes.flotteoceanographique.fr/series/243/. Last accessed 12/03/2021

Anonymous. 2018. Annual report to the commission - Part 1: information of fisheries, research, and statistics: New Caledonia. WCPFC Scientific Committee 14th regular session, Busan, Republic of Korea, 9-16 August 2018. Kolonia: Western and Central Pacific Fisheries Commission, SC14-AR/CCM-15.

Benoit-Bird KJ. 2009. The effects of scattering-layer composition, animal size, and numerical density on the frequency response of volume backscatter. ICES J Mar Sci 66:582–593.

Benoit-Bird KJ, Au WWL. 2003. Prey dynamics affect foraging by a pelagic predator (*Stenella longirostris*) over a range of spatial and temporal scales. Behav Ecol Sociobiol 53:364–373.

Benoit-Bird KJ, McManus MA. 2012. Bottom-up regulation of a pelagic community through spatial aggregations. Biol Lett 8:813–816.

Bertrand A, Bard F-X, Josse E. 2002a. Tuna food habits related to the micronekton distribution in French Polynesia. Mar Biol 140:1023–1037.

Bertrand A, Grados D, Colas F, Bertrand S, Capet X, Chaigneau A, Vargas G, Mousseigne A, Fablet R. 2014. Broad impacts of fine-scale dynamics on seascape structure from zooplankton to seabirds. Nature Comm 5:5239.

Bertrand A, Josse E, Bach P, Gros P, Dagorn L. 2002b. Hydrological and trophic characteristics of tuna habitat: consequences on tuna distribution and longline catchability. Can J Fish Aquat Sci 59:1002–1013.

Blanc P, Wald L. 2012. The SG2 algorithm for a fast and accurate computation of the position of the Sun for multi-decadal time period. Solar Energy 86:3072–3083.

Block BA, Jonsen ID, Jorgensen SJ, Winship AJ, Shaffer SA, Bograd SJ, Hazen EL, Foley DG, Breed GA, Harrison A-L, Ganong JE, Swithenbank A, Castleton M, Dewar H, Mate BR, Shillinger GL, Schaefer KM, Benson SR, Weise MJ, Henry RW, Costa DP. 2011. Tracking apex marine predator movements in a dynamic ocean. Nature 475:86–90.

Borsa P, Pandolfi M, Andréfouët S, Bretagnolle V. 2010. Breeding Avifauna of the Chesterfield Islands, Coral Sea: Current Population Sizes, Trends, and Threats. Pac Sci 64:297–314.

Borsa P, Vidal É. 2018. Fragile and threatened: the seabirds of the Coral Sea. In: Payri C.E., Ed. Nouvelle-Calédonie, archipel de corail. Marseille: Institut de recherche pour le développement, pp 135–140.

Boussarie G, Bakker J, Wangensteen OS, Mariani S, Bonnin L, Juhel J-B, Kiszka JJ, Kulbicki M, Manel S, Robbins WD, Vigliola L, Mouillot D. 2018. Environmental DNA illuminates the dark diversity of sharks. Sci Adv 4:eaap9661.

Briand K, Molony B, Lehodey P. 2011. A study on the variability of albacore (*Thunnus alalunga*) longline catch rates in the southwest Pacific ocean. Fisheries Oceanogr 20:517–529.

Brodie S, Jacox MG, Bograd SJ, Welch H, Dewar H, Scales KL, Maxwell SM. 2018. Integrating dynamic subsurface habitat metrics into species distribution models. Front Mar Sci 5:15.

Buckland ST, Anderson DR, Burnham KP, Laake JL, Borchers DL, Thomas L. 2001. Introduction to distance sampling: estimating abundance of biological populations. Oxford: Oxford University Press, 448 p.

Catry T, Ramos JA, Corre ML, Phillips RA. 2009. Movements, at-sea distribution and behaviour of a tropical pelagic seabird: the wedge-tailed shearwater in the western Indian Ocean. Mar Ecol Progr Ser 391:231–242.

Ceccarelli DM, McKinnon AD, Andréfouët S, Allain V, Young J, Gledhill DC, Flynn A, Bax NJ, Beaman R, Borsa P, Brinkman R, Bustamante RH, Campbell R, Cappo M, Cravatte S, D'Agata S, Dichmont CM, Dunstan PK, Dupouy C, Edgar G, Farman R, Furnas M, Garrigue C, Hutton T, Kulbicki M, Letourneur Y, Lindsay D, Menkes C, Mouillot D, Parravicini V, Payri C, Pelletier B, Richer de Forges B, Ridgway K, Rodier M, Samadi S, Schoeman D, Skewes T, Swearer S, Vigliola L, Wantiez L, Williams A, Williams A, Richardson AJ. 2013. The coral sea: physical environment, ecosystem status and biodiversity assets. Adv Mar Biol 66:213–290.

Choy CA, Haddock SHD, Robison BH. 2017. Deep pelagic food web structure as revealed by *in situ* feeding observations. Proc Roy Soc B Biol Sci 284:20172116.

Dagorn L, Holland KN, Hallier J-P, Taquet M, Moreno G, Sancho G, Itano DG, Aumeeruddy R, Girard C, Million J, Fonteneau A. 2006. Deep diving behavior observed in yellowfin tuna (*Thunnus albacares*). Aquat Living Resour 19:85–88.

Davison PC, Koslow JA, Kloser RJ. 2015. Acoustic biomass estimation of mesopelagic fish: backscattering from individuals, populations, and communities. ICES J Mar Sci 72:1413–1424.

Della Penna A, Gaube P. 2020. Mesoscale eddies structure mesopelagic communities. Front Mar Sci 7:454.

Derville S, Torres LG, Albertson R, Andrews O, Baker CS, Carzon P, Constantine R, Donoghue M, Dutheil C, Gannier A, Oremus M, Poole MM, Robbins J, Garrigue C. 2019. Whales in warming water: assessing breeding habitat diversity and adaptability in Oceania's changing climate. Global Change Biol 25:1466–1481.

Derville S, Torres LG, Zerbini AN, Oremus M, Garrigue C. 2020. Horizontal and vertical movements of humpback whales inform the use of critical pelagic habitats in the western South Pacific. Sci Rep 10:4871.

Doray M, Petitgas P, Romagnan JB, Huret M, Duhamel E, Dupuy C, Spitz J, Authier M, Sanchez F, Berger L, Dorémus G, Bourriau P, Grellier P, Massé J. 2018. The PELGAS survey: Ship-based integrated monitoring of the Bay of Biscay pelagic ecosystem. Progr Oceanogr 166:15–29.

Dormann C, McPherson J, Araújo M, Bivand R, Bolliger J, Carl G, Davies R, Hirzel A, Jetz W, Daniel Kissling W, Kühn I, Ohlemüller R, Peres-Neto P, Reineking B, Schröder B, Schurr F, Wilson R. 2007. Methods to account for spatial autocorrelation in the analysis of species distributional data: a review. Ecography 30:609–628.

Duffy LM, Olson RJ, Lennert-Cody CE, Galván-Magaña F, Bocanegra-Castillo N, Kuhnert PM. 2015. Foraging ecology of silky sharks, *Carcharhinus falciformis*, captured by the tuna purse-seine fishery in the eastern Pacific ocean. Mar Biol 162:571-593.

Dunn PK, Smyth GK. 1996. Randomized quantile residuals. J Comput Graphic Stat 5:236–244.

Escalle L, Gaertner D, Chavance P, Murua H, Simier M, Pascual-Alayón PJ, Ménard F, Ruiz J, Abascal F, Mérigot B. 2019. Catch and bycatch captured by tropical tuna purse-seine fishery in whale and whale shark associated sets: comparison with free school and FAD sets. Biodiv Conserv 28:467–499.

Escobar-Flores PC, O'Driscoll RL, Montgomery JC. 2018. Predicting distribution and relative abundance of mid-trophic level organisms using oceanographic parameters and acoustic backscatter. Mar Ecol Progr Ser 592:37–56.

Furukawa S, Tsuda Y, Nishihara GN, Fujioka K, Ohshimo S, Tomoe S, Nakatsuka N, Kimura H, Aoshima T, Kanehara H, Kitagawa T, Chiang W-C, Nakata H, Kawabe R. 2014. Vertical movements of Pacific bluefin tuna (*Thunnus orientalis*) and dolphinfish (*Coryphaena hippurus*) relative to the thermocline in the northern East China sea. Fisheries Res 149:86–91.

Gardes L, Tessier E, Allain V, Alloncle N, Baudat-Franceschi J, Butaud J-F, Collot J, Etaix-Bonnin R, Hubert A, Jourdan H, Loisier A, Menkes C, Payri C, Rouillard P, Samadi S, Vidal E, Yokohama Y. 2014. Analyse stratégique de l'espace maritime de la Nouvelle-Calédonie - vers une gestion intégrée. Nouméa: Agence des aires marines protégées, 470 p.

Garriga J, Palmer JRB, Oltra A, Bartumeus F. 2016. Expectation-Maximization binary clustering for behavioural annotation. PLoS One 11:e0151984.

Garrigue C, Clapham PJ, Geyer Y, Kennedy AS, Zerbini AN. 2015. Satellite tracking reveals novel migratory patterns and the importance of seamounts for endangered South Pacific humpback whales. Roy Soc Open Sci 2:150489.

Godo OR, Samuelsen A, Macaulay GJ, Patel R, Hjøllo SS, Horne J, Kaartvedt S, Johannessen JA. 2012. Mesoscale eddies are oases for higher trophic marine life. PLoS One 7:e30161.

Grados D, Bertrand A, Colas F, Echevin V, Chaigneau A, Gutiérrez D, Vargas G, Fablet R. 2016. Spatial and seasonal patterns of fine-scale to mesoscale upper ocean dynamics in an eastern boundary current system. Progr Oceanogr 142:105–116.

Green DB, Bestley S, Trebilco R, Corney SP, Lehodey P, McMahon CR, Guinet C, Hindell MA. 2020. Modelled mid-trophic pelagic prey fields improve understanding of marine predator foraging behaviour. Ecography 43:1014–1026.

Guinehut S, Dhomps A-L, Larnicol G, Le Traon P-Y. 2012. High resolution 3-D temperature and salinity fields derived from in situ and satellite observations. Ocean Sci Discuss 9:1313–1347.

Hastie T, Tibshirani R. 1990. Generalized additive models. London: Chapman & Hall, xv+335 p.

Houssard P, Lorrain A, Tremblay-Boyer L, Allain V, Graham BS, Menkes CE, Pethybridge H, Couturier LIE, Point D, Leroy B, Receveur A, Hunt BPV, Vourey E, Bonnet S, Rodier M, Raimbault P, Feunteun E, Kuhnert PM, Munaron J-M, Lebreton B, Otake T, Letourneur Y. 2017. Trophic position increases with thermocline depth in yellowfin and bigeye tuna across the western and central Pacific ocean. Progr Oceanogr 154:49–63.

Irigoien X, Klevjer TA, Røstad A, Martinez U, Boyra G, Acuña JL, Bode A, Echevarria F, Gonzalez-Gordillo JI, Hernandez-Leon S, Agusti S, Aksnes DL, Duarte CM, Kaartvedt S. 2014. Large mesopelagic fishes biomass and trophic efficiency in the open ocean. Nature Comm 5:3271.

Jaquemet S, Ternon JF, Kaehler S, Thiebot JB, Dyer B, Bemanaja E, Marteau C, Le Corre M. 2014. Contrasted structuring effects of mesoscale features on the seabird community in the Mozambique Channel. Deep Sea Res Pt II Topic Stud Oceanogr 100:200–211.

Kleiber P, Maunder MN. 2008. Inherent bias in using aggregate CPUE to characterize abundance of fish species assemblages. Fisheries Research 93:140–145.

Kleisner KM, Iii JFW, Diamond SL, Die DJ. 2010. Modeling the spatial autocorrelation of pelagic fish abundance. Mar Ecol Progr Ser 411:203–213.

Lambert C, Mannocci L, Lehodey P, Ridoux V. 2014. Predicting cetacean habitats from their energetic needs and the distribution of their prey in two contrasted tropical regions. PLoS One 9:e105958.

Lan K-W, Lee M-A, Chou C-P, Vayghan AH. 2018. Association between the interannual variation in the oceanic environment and catch rates of bigeye tuna (*Thunnus obesus*) in the Atlantic ocean. Fisheries Oceanogr 27:395–407.

Laran S, Hamani V, Authier M, Dorémus G, Van Canneyt O, Ridoux V, Watremez P. 2016. Distribution et abondance de la mégafaune marine dans le sud-ouest du Pacifique. Campagne REMMOA - Nouvelle-Calédonie et Wallis et Futuna. Rapport final, novembre 2016. La Rochelle: Observatoire Pelagis, 105 p.

Lehodey P, Maury O. 2010. CLimate Impacts on Oceanic TOp Predators (CLIOTOP): Introduction to the special issue of the CLIOTOP international symposium, La Paz, Mexico, 3–7 December 2007. Progr Oceanogr 86:1–7.

Lehodey P, Murtugudde R, Senina I. 2010. Bridging the gap from ocean models to population dynamics of large marine predators: A model of mid-trophic functional groups. Progr Oceanogr 84:69–84.

Lehodey P, Senina I, Sibert J, Hampton J. 2008. SEAPODYM v2: a spatial ecosystem and population dynamics model with parameter optimization providing a new tool for tuna management. WCPFC Scientific Committee 4th regular session, 11–22 August 2008, Port Moresby, Papua New Guinea. Kolonia: Western and Central Pacific Fisheries Commission, SC4-2008/EB-WP-10.

Leroy B, Peatman T, Usu T, Caillot S, Moore B, Williams A, Nicol S. 2016. Interactions between artisanal and industrial tuna fisheries: insights from a decade of tagging experiments. Mar Policy 65:11–9.

Lezama-Ochoa A, Boyra G, Goñi N, Arrizabalaga H, Bertrand A. 2010. Investigating relationships between albacore tuna (*Thunnus alalunga*) CPUE and prey distribution in the Bay of Biscay. Progr Oceanogr 86:105–114.

Lin S-J, Musyl MK, Wang S-P, Su N-J, Chiang W-C, Lu C-P, Tone K, Wu C-Y, Sasaki A, Nakamura I, Komeyama K, Kawabe R. 2019. Movement behaviour of released wild and farm-raised dolphinfish *Coryphaena hippurus* tracked by pop-up satellite archival tags. Fisheries Sci 85:779–790.

Lopez A, Pierce GJ, Santos MB, Gracia J, Guerra A. 2003. Fishery by-catches of marine mammals in Galician waters: results from on-board observations and an interview survey of fishermen. Biol Conserv 111:25–40.

Louzao M, García-Baró I, Rubio A, Martínez U, Vázquez JA, Murcia JL, Nogueira E, Boyra G. 2019a. Understanding the 3D environment of pelagic predators from multidisciplinary oceanographic surveys to advance ecosystem-based monitoring. Mar Ecol Progr Ser 617–618:199–219.

Louzao M, Pinaud D, Péron C, Delord K, Wiegand T, Weimerskirch H. 2011. Conserving pelagic habitats: seascape modelling of an oceanic top predator. J Appl Ecol 48:121–132.

Louzao M, Valeiras X, García-Barcelona S, González-Quirós R, Nogueira E, Iglesias M, Bode A, Vázquez JA, Murcia JL, Saavedra C, Pierce GJ, Fernández R, Garcí a-Barón I, Santos MB. 2019b. Marine megafauna niche coexistence and hotspot areas in a temperate ecosystem. Cont Shelf Res 186:77-87.

Maclennan DN, Fernandes PG, Dalen J. 2002. A consistent approach to definitions and symbols in fisheries acoustics. ICES J Mar Sci 59:365–369.

Mannocci L, Catalogna M, Dorémus G, Laran S, Lehodey P, Massart W, Monestiez P, Van Canneyt O, Watremez P, Ridoux V. 2014a. Predicting cetacean and seabird habitats across a productivity gradient in the South Pacific gyre. Progr Oceanogr 120:383–398.

Mannocci L, Laran S, Monestiez P, Dorémus G, Van Canneyt O, Watremez P, Ridoux V. 2014b. Predicting top predator habitats in the Southwest Indian Ocean. Ecography 37:261–278.

Mannocci L, Monestiez P, Spitz J, Ridoux V. 2015. Extrapolating cetacean densities beyond surveyed regions: habitat-based predictions in the circumtropical belt. J Biogeogr 42:1267–1280.

Marques FFC, Buckland ST. 2004. Covariate models for the detection function. In: Buckland ST, Anderson DR, Burnham KP, Laake JL, Borchers DL, Thomas L, eds. Advanced distance sampling. Oxford: Oxford University Press, 31-47.

Martin H, Lecren A. 2014. Arrêté n° 2014-1063/GNC du 23 avril 2014 créant le parc naturel de la mer de corail. J Off Nouv-Calédonie 9028:4245-4247.

McDuie F, Weeks S, Congdon B. 2018. Oceanographic drivers of near-colony seabird foraging site use in tropical marine systems. Mar Ecol Progr Ser 589:209–225.

McDuie F, Weeks SJ, Miller MG, Congdon BC. 2015. Breeding tropical shearwaters use distant foraging sites when self-provisioning. Mar Ornithol 43:123–129.

Mendez L, Borsa P, Cruz S, Grissac S de, Hennicke J, Lallemand J, Prudor A, Weimerskirch H. 2017. Geographical variation in the foraging behaviour of the pantropical red-footed booby. Mar Ecol Progr Ser 568:217–230.

Mendez L, Cotté C, Prudor A, Weimerskirch H. 2016. Variability in foraging behaviour of red-footed boobies nesting on Europa Island. Acta Oecol 72:87–97.

Mendez L, Prudor A, Weimerskirch H. 2020. Inter-population variation in the behaviour of adult and juvenile red-footed boobies *Sula sula*. Ibis 162:460–476.

Michalsky JJ. 1988. The Astronomical Almanac's algorithm for approximate solar position (1950–2050). Solar Energy 40:227–235.

Miller MGR, Carlile N, Phillips JS, McDuie F, Congdon BC. 2018. Importance of tropical tuna for seabird foraging over a marine productivity gradient. Mar Ecol Progr Ser 586:233–249.

Olson R, Duffy L, Kuhnert P, Galván-Magaña F, Bocanegra-Castillo N, Alatorre-Ramírez V. 2014. Decadal diet shift in yellowfin tuna *Thunnus albacares* suggests broad-scale food web changes in the eastern tropical Pacific Ocean. Mar Ecol Progr Ser 497:157–178.

Opdal AF, Godø OR, Bergstad OA, Fiksen Ø. 2008. Distribution, identity, and possible processes sustaining meso- and bathypelagic scattering layers on the northern mid-Atlantic ridge. Deep Sea Res Pt II Topic Stud Oceanogr 55:45–58.

Pandolfi-Benoit M, Bretagnolle V. 2002. Seabirds of the southern lagoon of New Caledonia; distribution, abundance and threats. Waterbirds 25:202–213.

Pérez-Jorge S, Tobeña M, Prieto R, Vandeperre F, Calmettes B, Lehodey P, Silva MA. 2020. Environmental drivers of large-scale movements of baleen whales in the mid-North Atlantic ocean. Divers Distrib 26:683–698.

Potier M, Marsac F, Cherel Y, Lucas V, Sabatie R, Maury O, Ménard F. 2007. Forage fauna in the diet of three large pelagic fishes (lancetfish, swordfish and yellowfin tuna) in the western equatorial Indian Ocean. Fisheries Research 83:60–72.

Proud R, Cox MJ, Brierley AS. 2017. Biogeography of the global ocean's mesopelagic zone. Curr Biol 27:113–119.

Proud R, Cox MJ, Le Guen C, Brierley AS. 2018. Fine-scale depth structure of pelagic communities throughout the global ocean based on acoustic sound scattering layers. Mar Ecol Progr Ser 598:35–48.

Proud R, Handegard NO, Kloser RJ, Cox MJ, Brierley AS. 2019. From siphonophores to deep scattering layers: uncertainty ranges for the estimation of global mesopelagic fish biomass. ICES J Mar Sci 76:718–733.

Putra MIH, Mustika PLK. 2020. Incorporating in situ prey distribution into foraging habitat modelling for marine megafauna in the Solor waters of the Savu Sea, Indonesia. Aquat Conserv Mar Freshw Ecosyst 30:2384–2401.

Ravache A, Bourgeois K, Thibault M, Dromzée S, Weimerskirch H, De Grissac S, Prudor A, Lorrain A, Menkès C, Allain V, Bustamante P, Letourneur Y, VIDAL E. 2020a. Flying to the moon: Lunar cycle influences trip duration and nocturnal foraging behavior of the wedge-tailed shearwater Ardenna pacifica. J Exp Mar Biol Ecol 525:151322.

Ravache A, Bourgeois K, Weimerskirch H, Pagenaud A, de Grissac S, Miller M, Dromzée S, Lorrain A, Allain V, Bustamante P, Bylemans J, Gleeson D, Letourneur Y, Vidal É. 2020b. Behavioral and trophic segregations help the Tahiti petrel to cope with the abundance of wedge-tailed shearwater when foraging in oligotrophic tropical waters. Sci Rep 10:15129.

Receveur A, Dutheil C, Gorgues T, Menkes C, Lengaigne M, Nicol S, Lehodey P, Allain V, Menard F, Lebourges-Dhaussy A. 2021. Exploring the future of the Coral Sea micronekton. Progr Oceanogr 195:102593.

Receveur A, Kestenare E, Allain V, Ménard F, Cravatte S, Lebourges-Dhaussy A, Lehodey P, Mangeas M, Smith N, Radenac M-H, Menkes C. 2020a. Micronekton distribution in the southwest Pacific (New Caledonia) inferred from shipboard-ADCP backscatter data. Deep Sea Res Pt I: Oceanogr Res Pap 159:103237.

Receveur A, Menkes C, Allain V, Lebourges-Dhaussy A, Nerini D, Mangeas M, Menard F. 2019. Seasonal and spatial variability in the vertical distribution of pelagic forage fauna in the southwest Pacific. Deep Sea Res Pt II Topic Stud Oceanogr 175:104655.

Receveur A, Vourey E, Lebourges Dhaussy A, Menkes C, Menard F, Allain V. 2020b. Biogeography of micronekton assemblages in the Natural Park of the Coral Sea. Front Mar Sci 7:449.

Reynolds RW, Smith TM, Liu C, Chelton DB, Casey KS, Schlax MG. 2007. Daily high-resolution-blended analyses for sea surface temperature. J Clim 20:5473–5496.

Robinson LM, Elith J, Hobday AJ, Pearson RG, Kendall BE, Possingham HP, Richardson AJ. 2011. Pushing the limits in marine species distribution modelling: lessons from the land present challenges and opportunities. Global Ecol Biogeogr 20:789–802.

Sabarros P, Ménard F, Lévénez J, Tew-Kai E, Ternon J. 2009. Mesoscale eddies influence distribution and aggregation patterns of micronekton in the Mozambique Channel. Mar Ecol Progr Ser 395:101–107.

Saulquin B, Gohin F, Garrello R. 2011. Regional objective analysis for merging high-resolution MERIS, MODIS/Aqua, and SeaWiFS chlorophyll- a data from 1998 to 2008 on the European Atlantic shelf. IEEE Trans Geosci Remote Sens 49:143–154.

Schaefer KM, Fuller DW. 2007. Vertical movement patterns of skipjack tuna (Katsuwonus pelamis) in the eastern equatorial Pacific Ocean, as revealed with archival tags. Fishery Bull 105:379–389.

Schaefer KM, Fuller DW. 2010. Vertical movements, behavior, and habitat of bigeye tuna (*Thunnus obesus*) in the equatorial eastern Pacific ocean, ascertained from archival tag data. Mar Biol 157:2625–2642.

Schaefer KM, Fuller DW, Block BA. 2009. Vertical movements and habitat utilization of skipjack (*Katsuwonus pelamis*), yellowfin (*Thunnus albacares*), and bigeye (*Thunnus obesus*) tunas in the equatorial eastern Pacific Ocean, ascertained through archival tag data. In: Nielsen JL, Arrizabalaga H, Fragoso N, Hobday A, Lutcavage M, Sibert J, eds. Tagging and tracking of marine animals with electronic devices. Reviews, methods and technologies in fish biology and fisheries. Dordrecht: Springer, pp 121–144.

Stewart HA, Jamieson AJ. 2018. Habitat heterogeneity of hadal trenches: Considerations and implications for future studies. Progr Oceanogr 161:47–65.

Teffer AK, Staudinger MD, Juanes F. 2015. Trophic niche overlap among dolphinfish and co-occurring tunas near the northern edge of their range in the western North Atlantic. Mar Biol 162:1823–1840.

Tew Kai E, Marsac F. 2010. Influence of mesoscale eddies on spatial structuring of top predators' communities in the Mozambique Channel. Progr Oceanogr 86:214–223.

Tew Kai E, Rossi V, Sudre J, Weimerskirch H, Lopez C, Hernandez-Garcia E, Marsac F, Garçon V. 2009. Top marine predators track Lagrangian coherent structures. Proc Natl Acad Sci USA 106:8245–8250.

Tirard P, Manning MJ, Jollit I, Duffy C, Borsa P. 2010. Records of great white sharks (*Carcharodon carcharias*) in New Caledonian waters. Pac Sci 64:567–576.

Torres LG, Read AJ, Halpin P. 2008. Fine-scale habitat modeling of a top marine predator: do prey data improve predictive capacity? Ecol Applic 18:1702–1717.

Weimerskirch H, Grissac S de, Ravache A, Prudor A, Corbeau A, Congdon BC, McDuie F, Bourgeois K, Dromzée S, Butscher J, Menkes C, Allain V, Vidal E, Jaeger A, Borsa P. 2020. At-sea movements of wedge-tailed shearwaters during and outside the breeding season from four colonies in New Caledonia. Mar Ecol Progr Ser 633:225–238.

Williams AJ, Allain V, Nicol SJ, Evans KJ, Hoyle SD, Dupoux C, Vourey E, Dubosc J. 2015. Vertical behavior and diet of albacore tuna (*Thunnus alalunga*) vary with latitude in the South Pacific ocean. Deep Sea Res Pt II Topic Stud Oceanogr 113:154–169.

Wood SN. 2006. Generalized additive models: an introduction with R. Boca Raton FL: CRC Press, 391+xviii p.

Wood SN. 2017. Generalized additive models: an introduction with R, 2nd edn. Boca Raton FL: CRC Press, 476 p.

Young JW, Lansdell MJ, Campbell RA, Cooper SP, Juanes F, Guest MA. 2010. Feeding ecology and niche segregation in oceanic top predators off eastern Australia. Mar Biol 157:2347–2368.

ZoNéCo. 2013. Atlas bathymétrique de la Nouvelle-Calédonie. Nouméa: Programme ZoNéCo pour une gestion durable des ressources marines de la Nouvelle-Calédonie.

Table 1. Predator variable summary indicating taxon, species code, logo used in figures, numbers of observations (N) with number of occurrences (i.e. when individuals were detected for cetaceans and when the behavior at the position was 'foraging' for seabirds), observation unit, data source, time of the day, sampling years (Y), and sampling months (M, with 1 to 12 indicating January to December)

Taxon	Code	Logo	N	Unit	Source	Time of the day	Y	M
Albacore tuna	ALB		14941	Number of sets with the number of fish caught per 100 hooks for each set	Longline Catch	*Unknown*	2010 to 2018	1 to 12
Yellowfin tuna	YFT		17420					
Dolphinfish	DOL		17106					
Delphininae	DELPH		3326 (39 sighting occurrences)	Number of 10km segment with the number of individuals counted for each segment	Aerial survey	Day	2014	10, 11 and 12
Globicep-halinae	GLOB		3247 (40 sighting occurrences)					
Ziphiidae	ZIPH		3238 (31 sighting occurrences)					
Wedge-tailed shearwater	WTSH		11679 (3934 feeding occurrences)	Number of GPS positions recorded for each foraging behavior ('feed', 'don't feed')	GPS tracking	Day and night	2017, 2018 and 2019	3 and 4
Tahiti petrel	TAPET		4624 (1586 feeding occurrences)				2017, 2018 and 2019	1, 6, 8 to 12
Red-footed boody	RFBO		6533 (1547 feeding occurrences)				2012 and 2015	5, 6 and 11

Table 2. Details of habitat distribution models tested: predator taxon, response variable, link function, distribution, offset to correct for sampling effort, explanatory variables other than the nautical area scattering coefficient (NASC), NASC variable, and details of the nested model. See Table 1 for taxon codes. *SST*: sea surface temperature; *d20*: depth of the 20°C isotherm; *bathy*: bathymetry

Taxon	Response variable	Link function	Distribution	Offset	Explanatory variables	NASC variable	Nested model
ALB	Number of fish caught	log	Negative binomial	Log(number of hooks)	SST, log of chlorophyll, d20, bathy, year, (lon,lat)	NASC$_{day\_night}$ by layer (epi, up_meso, low_meso)	Random effect by vessel
YFT	Number of fish caught	log	Negative binomial	Log(number of hooks)	SST, log of chlorophyll, d20, bathy, year, (lon,lat)	NASC$_{day\_night}$ by layer (epi, up_meso)	Random effect by vessel
DOL	Number of fish caught	log	Negative binomial	Log(number of hooks)	SST, log of chlorophyll, d20, bathy, year, (lon,lat)	NASC$_{day\_night}$ by layer (epi)	Random effect by vessel
DELPH, GLOB and ZIPH	Animal count	log	Tweedie	Log(sampled surface)	SST, log of chlorophyll, d20, bathy	NASC$_{day}$ by layer (epi, up_meso, low_meso)	-
WTSH, TAPET and RFBO	Foraging occurence	log	Binomial	-	SST, log of chlorophyll, d20, bathy	NASC$_{day\_10\text{-}30m}$ by moment (day, night)	Random effect by individual with autocorrelation

Table 3. Total deviance explained (second column) by predator abundance/occurrence models and for the five explanatory variables ordered by the importance of their influence. Italics indicate non-significant variables and bold names emphasize NASC's rank

Predator	Total deviance explained (%)	Explanatory variables in decreasing order of importance (deviance explained in %)				
ALB	22.7	SST	Bathymetry	D20	Chlorophyll	**NASC**
		10.6	9.8	9.4	2.4	**1.1**
YFT	18.5	Chlorophyll	Bathymetry	**NASC**	D20	SST
		15.3	6.8	**5.6**	0.7	0.1
DOL	28.2	Chlorophyll	SST	Bathymetry	**NASC**	*D20*
		17.4	2.9	1.1	**0.7**	*0.1*
DELPH	7.3	SST	Chlorophyll	*D20*	*Bathymetry*	***NASC***
		4.2	2.8	*0.6*	*0.2*	***0.01***
GLOB	31.7	D20	Chlorophyll	SST	Bathymetry	***NASC***
		14.8	7.1	5.5	3.2	***0.1***
ZIPH	26	Chlorophyll	D20	SST	Bathymetry	***NASC***
		8.5	6.2	6.7	3.7	***0.01***
WTSH	19.1	Bathymetry	**NASC**	D20	SST	Chlorophyll
		11.5	**6.7**	1.5	0.6	0.2
TAPET	26.2	Bathymetry	Chlorophyll	***NASC***	*SST*	*D20*
		24.3	4.8	***0.6***	*0.2*	*0.08*
RFBO	30.1	Bathymetry	**NASC**	SST	*D20*	*Chlorophyll*
		14.9	**5.7**	4.2	*0.6*	*0.07*
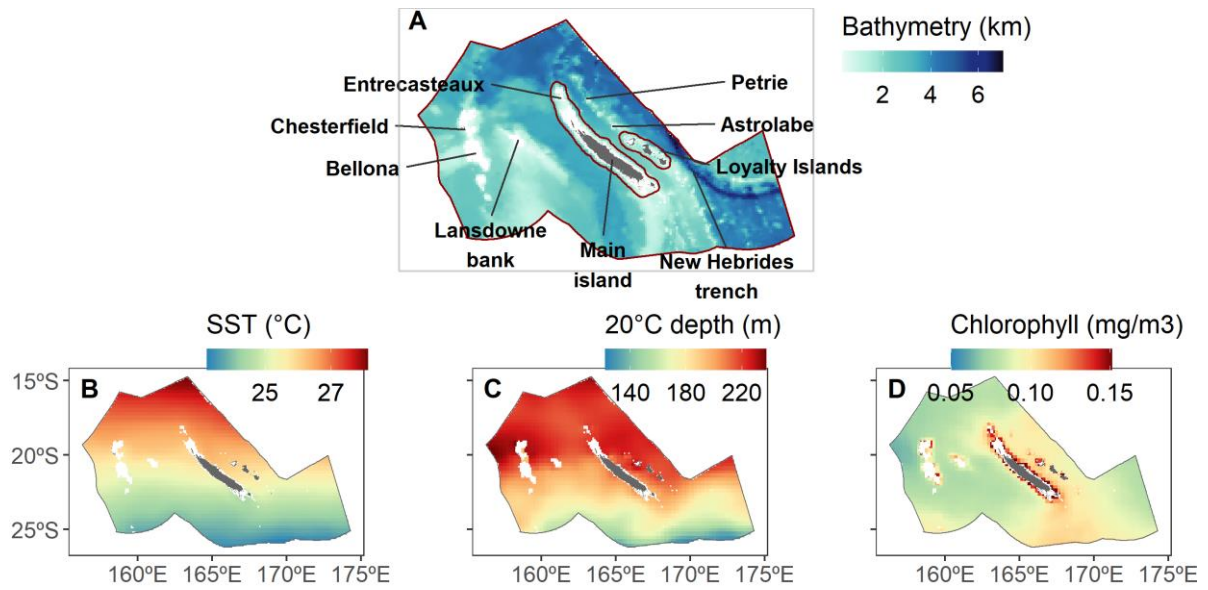
Figure 1. Spatial distribution of environmental covariates across the New Caledonia EEZ averaged across the 2010-2019 period. Land is represented in grey and white areas are waters with a bathymetry shallower than 300m. Data sources are given in SupplementaryTable S1. **A** bathymetry (in km). **B** Sea surface temperature (SST, in °C). **C** Depth of the 20°C isotherm (in m). **D** chlorophyll-a concentration (in mg.m^{-3}).
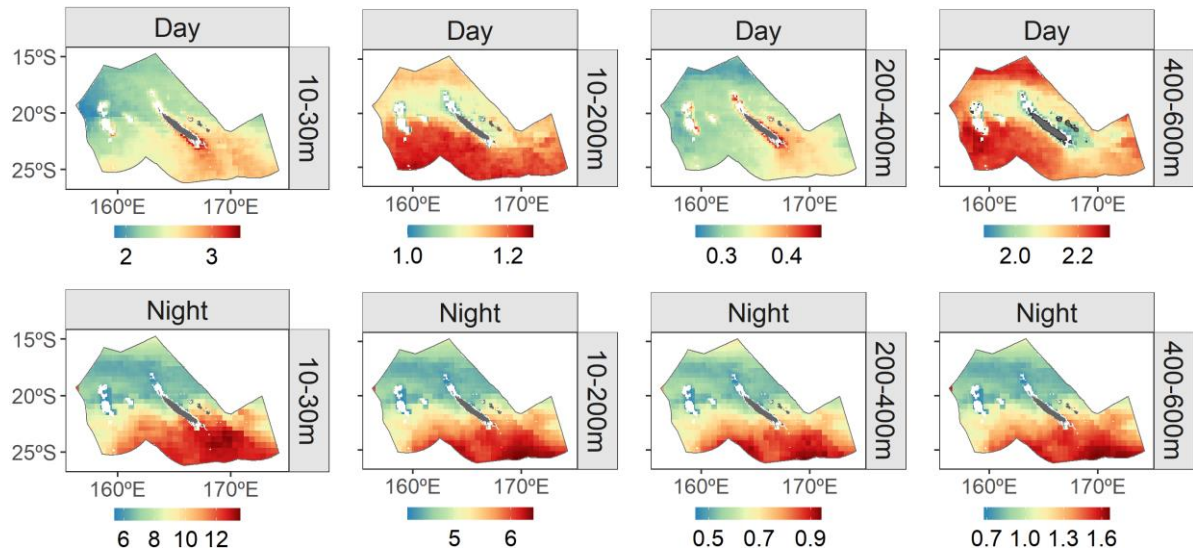
Figure 2. Spatial distribution of micronekton biomass index NASC (nautical area scattering coefficient) values (in m^2/nmi^2) during the day (top row), and during the night (bottom row) integrated over four vertical layers and on average for the 2010-2019 period: 10-30 m (sub-surface, first column), 10-200 m (epipelagic, second column), 200-400 m (upper mesopelagic, third column), and 400-600 m (lower mesopelagic, fourth column) across the New Caledonian EEZ. Color scale is different among panels. Land is represented in grey and white areas are waters with bathymetry shallower than 300 m.
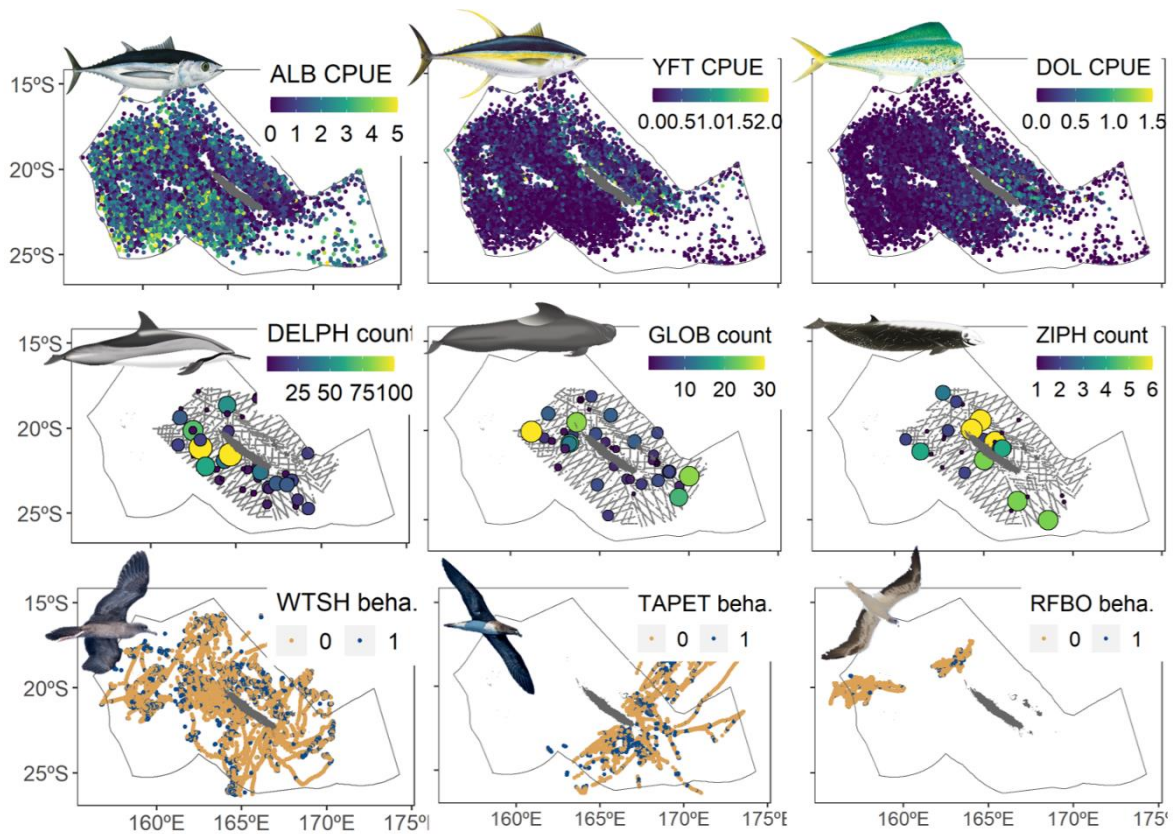
Figure 3. Raw data for the nine predators included in the study. Top row: catch per unit of effort (CPUE: number of fish caught per 100 hooks) for albacore (ALB), yellowfin tuna (YFT) and dolphinfish (DOL). Middle row: counts (grey points show absence of sighting) of Delphininae (DELPH), Globicephalinae (GLOB) and Ziphiidae (ZIPH, see section 2.1 for details on species). Bottom row: foraging (0: don't eat and 1: eat) behaviour positions obtained from GPS loggers in wedge-tailed shearwater (WTSH), Tahiti petrel (TAPET) and red-footed booby (RFBO). Seabird breeding sites are given in Supplementary Figure S2. Credit: © Les Hata, SPC (fish), © Youngmi Choi, SPC (cetacean), © Tubenoses Project, Hadoram Shirihai (WTSH and TAPET) and © Andreas Ravache, IRD (RFBO). Land is represented in grey.
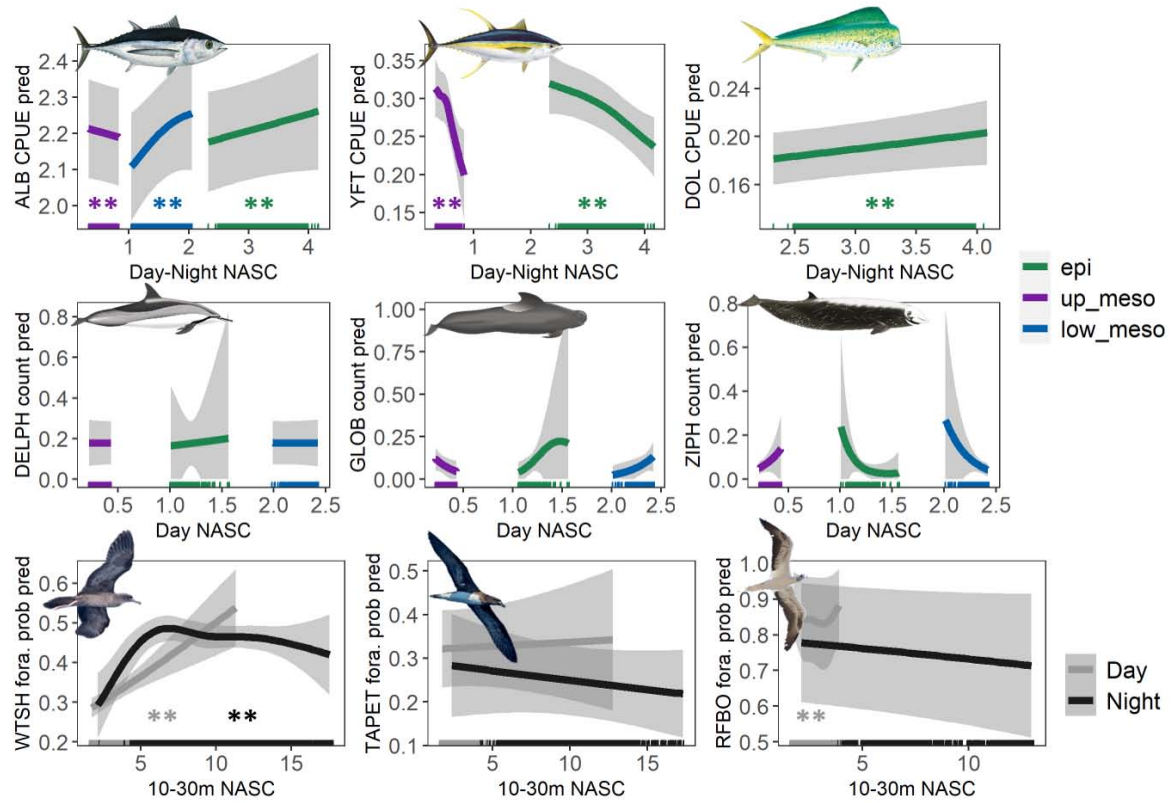
Figure 4. Modelled responses to the prey biomass index NASC (nautical area scattering coefficient, in m^2/nmi^2) variations: CPUE for tunas and dolphinfish, counts of individuals for cetaceans, and foraging probability for seabirds. Colors indicate different vertical layers of prey for tuna and cetaceans, and different times of day for seabirds. Solid grey ribbons correspond to the confidence limits ($\pm$ 2SE) of the model. Stars colored by the factor (vertical layer or moment) indicate significant relationships (p-value< 0.01). The ticks on the x-axis indicate the position of the observed values. Species codes on the y-axis are detailed in Table 1. © Les Hata, SPC (fish), © Youngmi Choi, SPC (cetacean), © Hadoram Shirihai/The Tubenoses Project, (WTSH and TAPET) and © Andreas Ravache, IRD (RFBO).
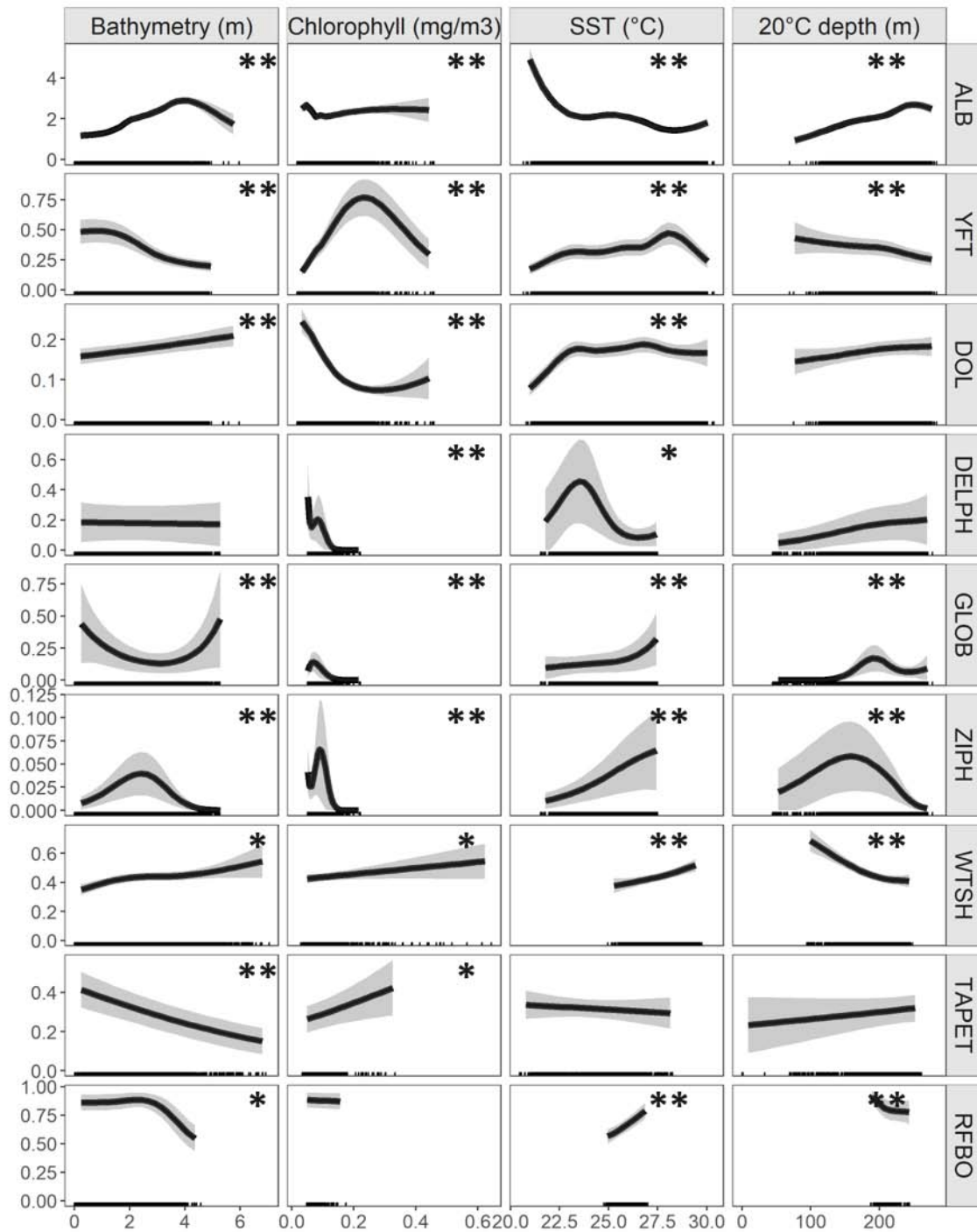
Figure 5. Modelled responses of predators (by row) to four environmental variables (by column). The solid grey ribbons correspond to the confidence limits of the model (± 2SE). Stars indicate the significance level: ** indicates highly significant (p-value < 0.01), * indicates slightly significant (0.01 < p-value < 0.1). The ticks on the x-axis indicate the observed values' position. Species codes are detailed in Table 1.
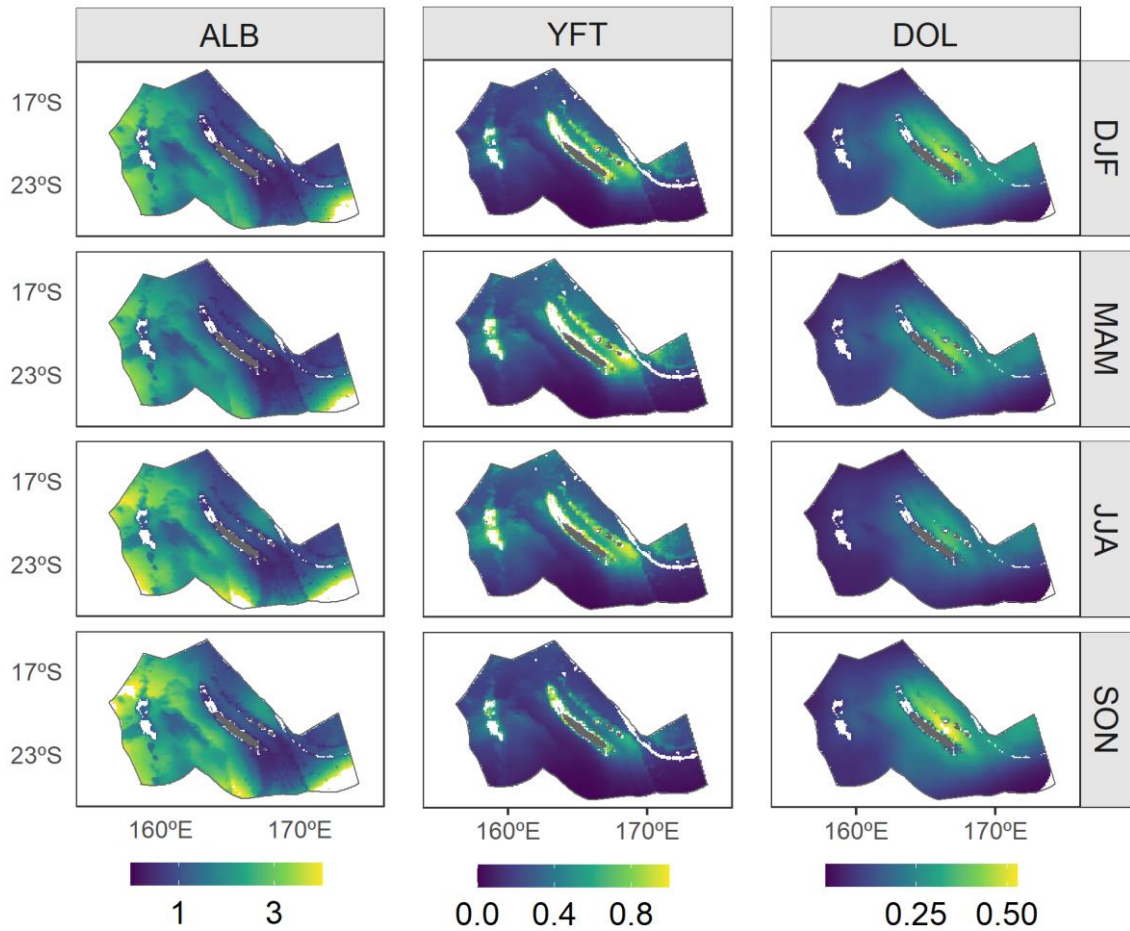
Figure 6. Spatial predictions of fish abundance index by quarter in the New Caledonia EEZ: catch per unit of effort (CPUE; number of fish caught per 100 hooks) of albacore (ALB), yellowfin tuna (YFT) and dolphinfish (DOL), with different scales according to species, and on average for the 2010-2019 period. DJF: December, January and February; MAM: March, April and May; JJA: June, July and August; SON: September, October and November. For each quarter, the three months were used for making predictions, as all months were sampled. Land is represented in grey. Reef and island names are indicated in Figure 1A. White areas (excepting waters with bathymetry shallower than 300 m identified in Figure 1) have no predictions because no extrapolation was performed.
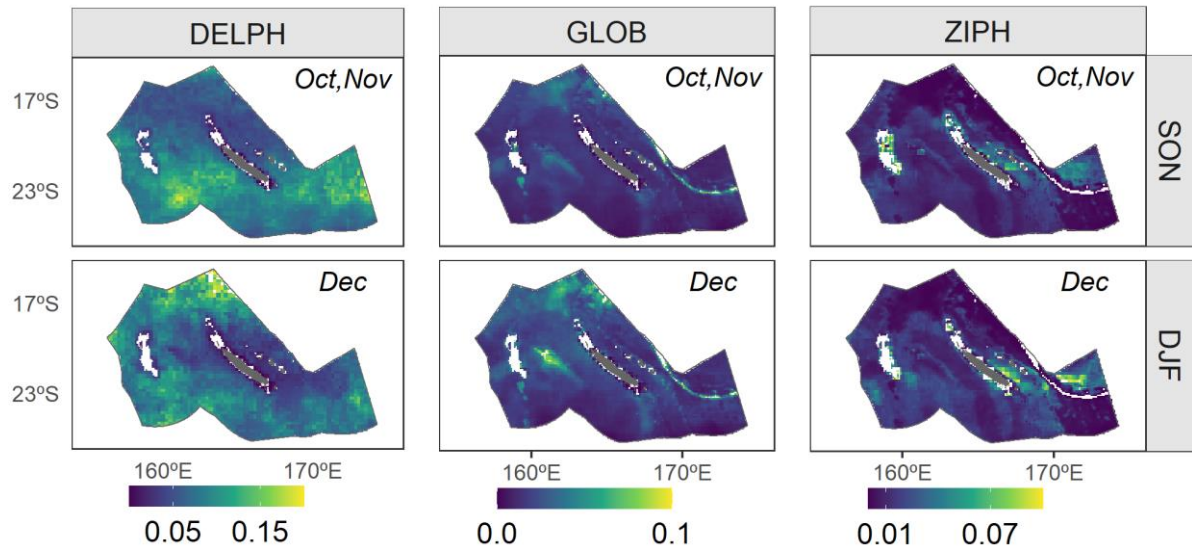
Figure 7. Spatial predictions of cetacean abundance by quarter in the New Caledonian EEZ: individual counts of Delphininae (DELPH), Globicephalinae (GLOB) and Ziphiidae (ZIPH), with different scales according to species, and on average for the 2010-2019 period. DJF: December, January and February; MAM: March, April and May; JJA: June, July and August; SON: September, October and November. Italic months in the right top corners indicate the sampled month and therefore the month used to do predictions. Reef and island names are indicated in Figure 1A. White areas (excepting waters with bathymetry shallower than 300 m identified in Figure 1) have no predictions because no extrapolation was performed.
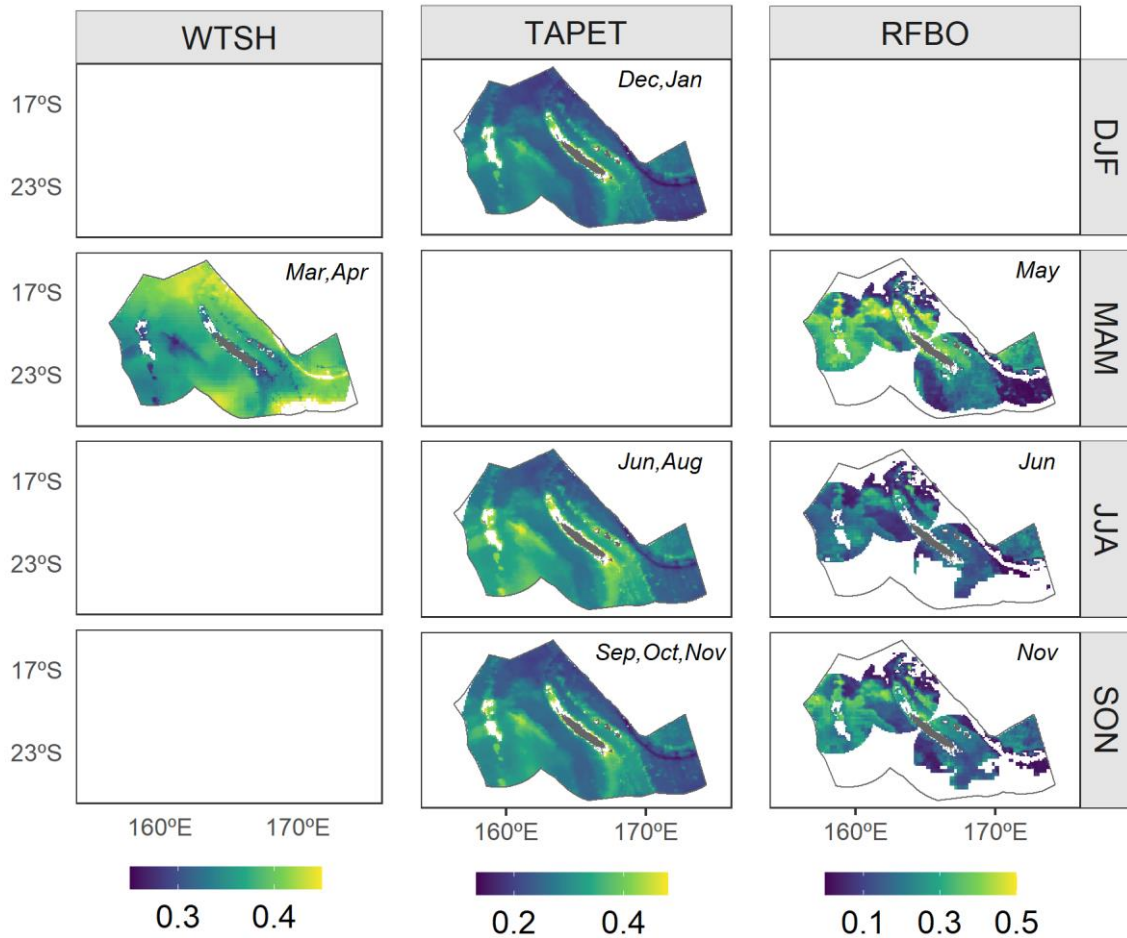
Figure 8. Spatial predictions of seabirds foraging probability by quarter in the New Caledonian EEZ: foraging occurrence of wedge-tailed shearwaters (WTSH), Tahiti petrels (TAPET) and red-footed boobies (RFBO), with different scales according to species, and on average for the 2010-2019 period. DJF: December, January and February; MAM: March, April and May; JJA: June, July and August; SON: September, October and November. Italic months in the right top corners indicate the sampled month and therefore the month used to do predictions. Reef and island names are indicated in Figure 1A. White areas (excepting waters with bathymetry shallower than 300m identified in Figure 1) have no predictions because no extrapolation was performed.

Supplementary Table S1. Summary of environmental variables used for the predator distribution models. Unit, source and resolution are detailed for each variable. NASC: nautical area scattering coefficient

Variable	Unit	Source	Temporal resolution	Spatial resolution
Bathymetry	km	ZoNéCo, 2013	-	500 m
Sea surface temperature	°C	Advanced very high-resolution radiometer (AVHRR) infrared satellite	Week	¼ degree
Chlorophyll-a	mg/m³	GlobColour-processor versions : MODIS 2014.0.1/VIIRSN 2014.0.2	Week	¼ degree
Depth of the 20°C isotherm	m	ARMOR3D	Week	¼ degree
NASC (prey biomass index proxy)	m²/nmi²	Receveur et al., 2019	Week	¼ degree

Supplementary Table S2. Seabird population size estimates (in breeding pairs) by geographic ensemble in New Caledonia

Geographic ensemble	Species		
	Ardenna pacifica (WTSH)	*Pseudobulweria rostrata* (TAPET)	*Sula sula* (RFBO)
Chesterfield-Bampton & Bellona	113 265 [a]	-	8 800 [a]
D'Entrecasteaux	4 176 [b]	-	2 883 [b]
Northern lagoon	35 573 [c]	1 [c]	-
Grande Terre	22 700 [d]	1 000 - 5 000 [h]	-
Southern lagoon	500 000 [e]	100 [e]	18 [e]
Loyalty Islands	1 410 - 1 660 [f]	5 [f]	> 12 [f]
Walpole	-	-	4 300 [j]
Matthew & Hunter	275 [g]	-	810 [g]
Total for New Caledonia	> 677 399	> 15 000 [i]	> 16 820

[a] Borsa P. 2019. Sites prioritaires pour la conservation des oiseaux marins et des tortues marines des atolls Chesterfield-Bampton et Bellona. Institut de recherche pour le développement, Nouméa, 28 p., https://hal.archives-ouvertes.fr/ird-02049265

[b] Robinet O., Sirgouant S., Bretagnolle V. 1997. Marine birds of d'Entrecasteaux Reefs (New Caledonia, southwestern Pacific): diversity, abundance, trends and threats. Colonial Waterbirds 20:282-290.

[c] Baudat-Franceschi J., Spaggiari J., Barré N. 2013. Oiseaux nicheurs d'intérêt pour la conservation.RAP Bulletin of Biological assessment 53:136-142.**,** http://www.bioone.org/doi/full/10.1896/054.053.0114

[d] Weimerskirch H., de Grissac S., Ravache A., Prudor A., Corbeau A., Congdon B.C., McDuie F., Bourgeois K., Dromzée S., Butscher J., Menkes C., Allain V., Vidal E., Jaeger A., Borsa P. 2020. At-sea movements of wedge-tailed shearwaters during and outside the breeding season from four colonies in New Caledonia. Marine Ecology Progress Series 633:225–238. doi: 10.3354/meps13171

[e] Pandolfi-Benoit M., Bretagnolle V. 2002. Seabirds of the southern lagoon of New Caledonia: distribution, abundance and threats. Waterbirds 25:202-213.

[f] Barré N., Villard P., Manceau N., Monimeau L., Ménard C. 2006. Les oiseaux de l'archipel des Loyauté (Nouvelle-Calédonie) : Inventaire et éléments d'écologie et de biogéographie. Revue d'Écologie (Terre et Vie) 61:175-194.

[g] Borsa P., Baudat-Franceschi J. 2019. Synthèse des observations sur l'avifaune marine des îles Matthew et Hunter (Parc naturel de la mer de Corail), 1973-2018. Institut de recherche pour le développement, Nouméa, 41 p., https://hal.ird.fr/ird-02300763

[h] Villard P., Dano S., Bretagnolle V. 2006. Morphometrics and the breeding biology of the Tahiti Petrel *Pseudobulweria rostrata*. Ibis 148:285-291.

[i] Borsa P. 2008. Mission ornithologique à l'îlot Loop (îles Chesterfield) et transects en mer de Corail et dans le bassin des Loyauté, 20-28 octobre 2008. Institut de recherche pour le développement, Nouméa, 13 p., doi: 10.23708/fdi:010045367

[j] Baudat-Franceschi J., Bachy P. 2013. Inventaire ornithologique de Walpole, mission du 13 au 23 mai 2013. Société calédonienne d'ornithologie, Nouméa, 24 p.
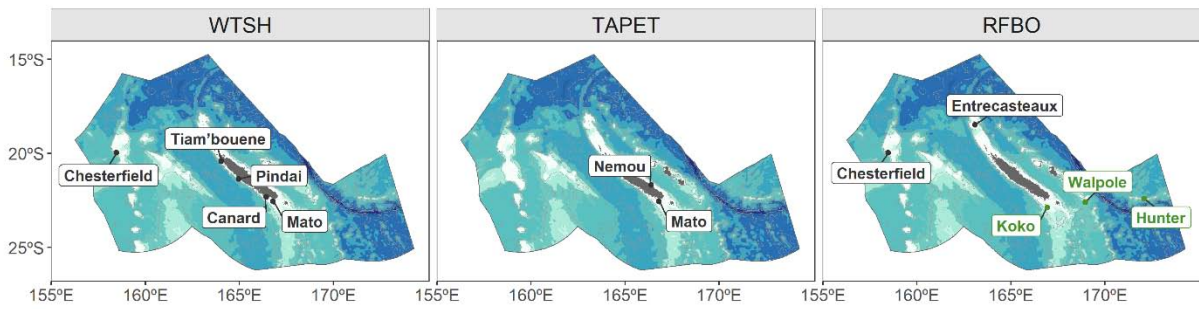
Supplementary Figure S2. Breeding sites of the GPS-tracked seabirds sampled in the present study in black (WTSH: Wedge-tailed shearwater; TAPET: Tahiti petrel; RFBO: Red-footed booby). Green points and names indicate the none-sampled but known RFBO colonies that are used for the spatial predictions.

Supplementary Table S3. Cruise details, with the cruise name, dates, the number of 0.1nm bins per cruise, and the d.o.i. of each cruise

Cruise name	Start	End	Number of 0.1 nm bins	d.o.i.
Nectalis1 (N1)	30/07/2011	15/08/2011	3681	10.17600/11100050
Nectalis2 (N2)	26/11/2011	14/12/2011	2896	10.17600/11100070
Nectalis3 (N3)	21/11/2014	08/12/2014	3617	10.17600/14004900
Nectalis4 (N4)	19/10/2015	25/10/2015	1034	10.17600/15004000
Nectalis5 (N5)	23/11/2016	06/12/2016	3989	10.17600/16004200
Puffalis (PUFF)	18/03/2017	31/03/2017	1498	10.17600/17003300
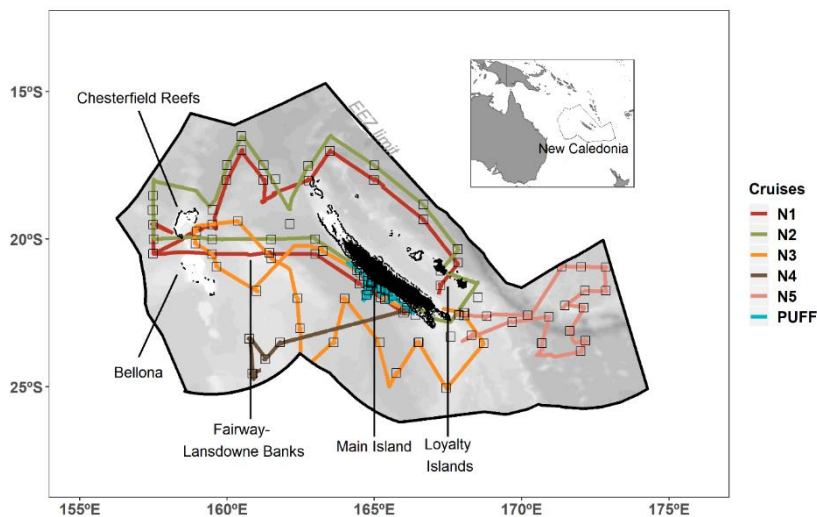
Supplementary Figure S3. Cruise tracks of the R/V *Alis* with EK60 echosounder (colored lines) in the New Caledonian exclusive economic zone. Black boxes show CTD stations. The background grey colors represent the relative seabed depth (where lighter colors are shallower). Note that N1 and N2 tracks partially overlap but N2 track has been slightly shifted to the north for visualization purposes.
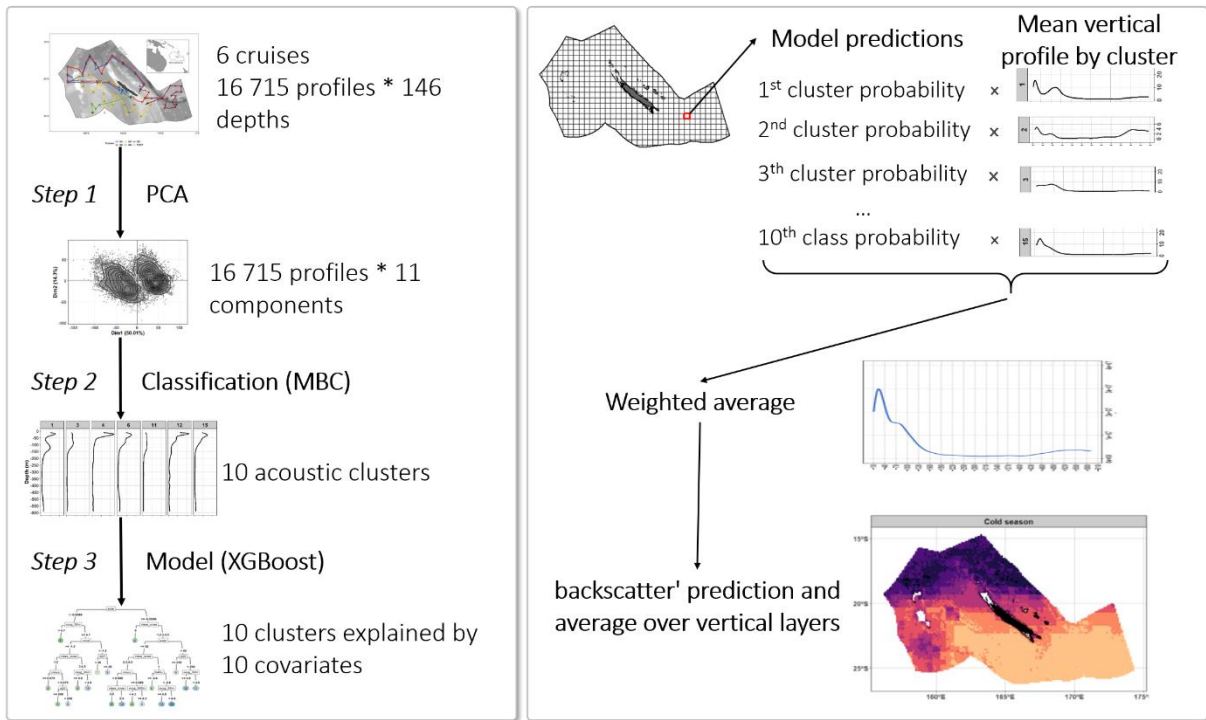
Supplementary Figure S4. Diagram explaining the different steps of the analysis.
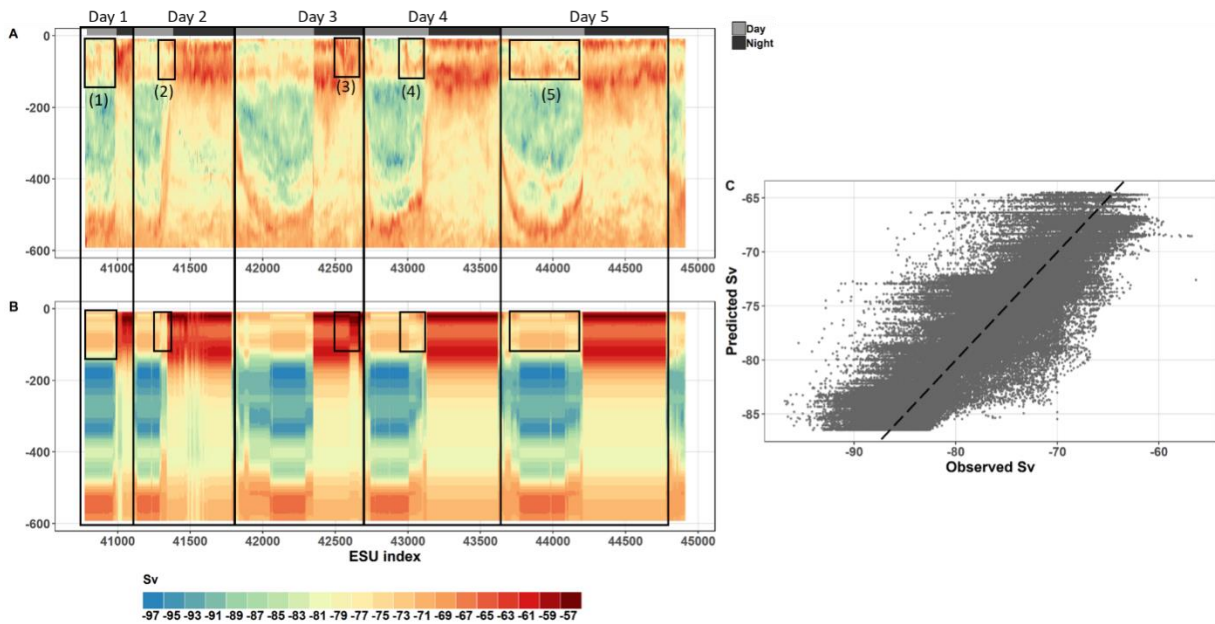
Supplementary Figure S5. N4 echogram observed (panel A) and predicted (panel B). Scatter plot of predicted values as a function of observed values with y = x dashed line over all data of N4 (panel C). Boxes drawn on the plots are discussed in the main text as box (1), (2), etc.

SUPPLEMENT 3 – R CODE

```r
library(ggplot2)
library(mgcv)
library(dplyr)

################################################################################
############################## Data loading ####################################
########### Fishes datasets (logbook of NC longliners) ###########
load(file = 'C:/df_ALB.Rdata')
load(file = 'C:/df_YFT.Rdata')
load(file = 'C:/df_DOL.Rdata')

summary(df_ALB)

## n_ALB_caught     n_hook        year           month
## Min.  : 0.00   Min.  : 175   Min.  :2010   Min.  : 1.000
## 1st Qu.:12.00  1st Qu.:1800  1st Qu.:2012   1 st Qu.: 4.000
## Median :30.00  Median :2000  Median :2015   Median : 6.000
## Mean  :39.15   Mean  :1964   Mean  :2014   Mean  : 6.454
## 3rd Qu.:57.00  3rd Qu.:2100  3rd Qu.:2017   3rd Qu.: 9.000
## Max.  :198.00  Max.  :4450   Max.  :2018   Max.  :12.000
##     day        vessel_code       lon            lat
## Min.  : 1.05   1248 : 8034   Min.  :156.9   Min.  :-25.65
## 1st Qu.: 8.02  0211 : 7638   1st Qu.:160.3  1st Qu.:-22.13
## Median :16.05  7430 : 5598   Median :162.6  Median :-21.03
## Mean  :15.72   2761 : 5460   Mean  :162.6   Mean  :-21.00
## 3rd Qu.:23.05  7350 : 5220   3rd Qu.:164.6  3rd Qu.:-19.97
## Max.  :31.0    (Other):12873  Max.  :172.6  Max.  :-14.85
##     bathy          SST          chloro           d20
## Min.  :0.00396  Min.  :20.65  Min.  :0.01688  Min.  :69.16
## 1st Qu.:1.98710 1st Qu.:24.27 1st Qu.:0.05962 1st Qu.:191.32
## Median :2.39458 Median :25.61 Median :0.07996 Median :208.98
## Mean  :2.53872  Mean  :25.57  Mean  :0.09147  Mean  :207.60
## 3rd Qu.:3.37107 3rd Qu.:26.92 3rd Qu.:0.11350 3rd Qu.:226.49
## Max.  :5.95959  Max.  :30.37  Max.  :0.58071  Max.  :283.39
##     NASC         vertical_layer
## Min.  :0.3300    Epi:14941
## 1st Qu.:0.5336      Upper_meso:14941
## Median :1.5905      Lower_meso:14941
## Mean  :1.7010
## 3rd Qu.:2.7181
## Max.  :4.1644
df_ALB$log_chloro <- log(df_ALB$chloro + 1)
## the two other fish datasets are built in the same way.
########### Cetaceans datasets (REMMOA survey) ###########
load(file = 'C:/df_DELPH.Rdata')
load(file = 'C:/df_GLOB.Rdata')
load(file = 'C:/df_ZIPH.Rdata')

summary(df_DELPH)

## n_individuals  transect_length    year          month
## Min.  : 0.00   Min.  : 175     Min.  :2014   Min.  :10.00
## 1st Qu.:12.00  1st Qu.:1800    1st Qu.:2014  1st Qu.:10.00
## Median :30.00  Median :2000    Median :2014  Median :11.00
## Mean  :39.15   Mean  :1964     Mean  :2014   Mean  :10.82
## 3rd Qu.:57.00  3rd Qu.:2100    3rd Qu.:2014  3rd Qu.:11.00
## Max.  :198.00  Max.  :4450     Max.  :2014   Max.  :12.00
##     day          ESW           lon            lat
## Min.  : 1.0    Min.  :0.199   Min.  :160.2   Min.  :-25.39
## 1st Qu.:12.0   1st Qu.:0.200  1st Qu.:163.6  1st Qu.:-22.81
## Median :17.0   Median :0.200  Median :165.4  Median :-21.38
## Mean  :18.1    Mean  :0.204   Mean  :165.5   Mean  :-21.38
##3rd Qu.:27.0    3rd Qu.:0.216  3rd Qu.:167.4  3rd Qu.:-19.93
## Max.  :31.0    Max.  :0.254   Max.  :171.0   Max.  :-17.63
##     bathy          SST          chloro           d20
## Min.  :0.002   Min.  :21.53   Min.  :0.03971  Min.  :44.62
## 1st Qu.:1.579  1st Qu.:23.64  1st Qu.:0.05968 1st Qu.:190.17
## Median :2.574  Median :25.15  Median :0.06823 Median :218.53
## Mean  :2.527   Mean  :25.13   Mean  :0.07534  Mean  :207.38
## 3rd Qu.:3.519  3rd Qu.:26.33  3rd Qu.:0.08181 3rd Qu.:236.03
## Max.  :4.943   Max.  :28.67   Max.  :0.24861  Max.  :277.47
##     NASC         vertical_layer
## Min.  :0.2178    Epi:15079
## 1st Qu.:0.2766   Upper_meso:15079
```

```
## Median :1.2326   Lower_meso:15079
## Mean  :1.2701
## 3rd Qu.:2.2815
## Max.  :2.4965
df_DELPH$surface <- 2 *df_DELPH$transect_length *df_DELPH$ESW
## the two other cetacean datasets are built in the same way.
########## Seabirds datasets (tracking) ##########
load(file = 'C:/df_WTSH.Rdata')
load(file = 'C:/df_TAPET.Rdata')
load(file = 'C:/df_RFBO.Rdata')

summary(df_WTSH)

## foraging_behaviour foraging_factor foraging_numeric       year
## commuting :6030   Dont eat:10402  Min.  :0.0000   Min.  :2017
## DD     : 52   Eat   : 7070  1st Qu.:0.0000   1st Qu.:2017
## foraging :7070              Median :0.0000   Median :2017
## resting  :4320              Mean  :0.4046   Mean  :2018
##                             3rd Qu.:1.0000   3rd Qu.:2019
##                             Max.  :1.0000   Max.  :2019
##     month       day       lon       lat       hour
## Min. :3.0  Min.  : 1.0  Min.  :156.8  Min.  :-26.3  Length:17472
## 1st Qu.:3.0  1st Qu.: 7.0  1st Qu.:160.5  1st Qu.:-21.2  Class :char
## Median :4.0  Median :13.0  Median :164.5  Median :-20.3  Mode :char
## Mean :3.7  Mean  :11.9  Mean  :163.7  Mean  :-20.4
## 3rd Qu.:4.0  3rd Qu.:17.0  3rd Qu.:166.3  3rd Qu.:-19.2
## Max. :4.0  Max.  :27.0  Max.  :170.4  Max.  :-15.6
##    bathymetry       SST       chlorophyll       d20
## Min.  :0.0004   Min.  :24.96  Min.  :0.02971   Min.  :94.28
## 1st Qu.:1.8990  1st Qu.:26.82  1st Qu.:0.09709   1st Qu.:179.53
## Median :2.6146  Median :27.70  Median :0.11071  Median :197.03
## Mean  :2.6503  Mean  :27.61  Mean  :0.12411   Mean  :195.08
## 3rd Qu.:3.5237  3rd Qu.:28.44  3rd Qu.:0.13703   3rd Qu.:213.84
## Max.  :7.0341   Max.  :29.75  Max.  :0.60467   Max.  :248.29
##    NASC        moment       Individu
## Min.  :1.596  Day :8737   FS101257: 777
## 1st Qu.: 2.655  Night:8735   FS101268: 589
## Median :4.188              FS101280: 546
## Mean  :6.192              FS101212: 530
## 3rd Qu.:9.708              FS107228:492
## Max.  :17.766          (Other) :8745
## the two other seabird datasets are built in the same way.
###########################################################################
################################### Modelling ###################################
#### ALBACORE
model_alb<- gam(n_ALB ~ offset(n_hook) +
            s(NASC, k = 24, bs = "cr", by = vertical_layer) +
            s(SST, k = 8, bs = "cr") +
            s(log_chloro, k = 8, bs = "cr") +
            s(d20, k = 8, bs = "cr") +
            s(bathy, k = 8, bs = "cr") +
            s(year, k = 8, bs = "cr") +
            s(vessel_code, bs = "re") +
            s(lon, lat, bs = 'gp', k = 30),
            gamma= 1.4,
            data= df_ALB,
            family=nb(link ='log'),
            method="REML")
#### YELLOWFIN
model_yft<- gam(n_YFT ~ offset(n_hook) +
            s(NASC, k = 24, bs = "cr", by = vertical_layer) +
            s(SST, k = 8, bs = "cr") +
            s(log_chloro, k = 8, bs = "cr") +
            s(d20, k = 8, bs = "cr") +
            s(bathy, k = 8, bs = "cr") +
            s(year, k = 8, bs = "cr") +
            s(vessel_code, bs = "re") +
            s(lon, lat, bs = 'gp', k = 30),
            gamma= 1.4,
            data= df_YFT,
            family=nb(link ='log'),
            method="REML")
#### DOLPHINFISH
model_dol<- gam(n_DOL ~ offset(n_hook) +
            s(NASC, k = 24, bs = "cr", by = vertical_layer) +
            s(SST, k = 8, bs = "cr") +
            s(log_chloro, k = 8, bs = "cr") +
```

```
                s(d20, k = 8, bs = "cr") +
                s(bathy, k = 8, bs = "cr") +
                s(year, k = 8, bs = "cr") +
                s(vessel_code, bs = "re") +
                s(lon, lat, bs = 'gp', k = 30),
                gamma= 1.4,
                data= df_DOL,
                family=nb(link ='log'),
                method="REML")
#### DELPHINAE
model_delph = gam(n_individuals ~ offset(log_surface) +
                s(NASC, k = 16, bs = "cr", by = vertical_layer) +
                s(SST, k= 8, bs= "cr") +
                s(log_chloro, k = 8, bs = "cr") +
                s(d20, k = 8, bs= "cr") +
                s(bathy,k = 8, bs= "cr"),
                family= tw(link ='log'),
                method= "REML",
                data= df_DELPH)
#### GLOBICEPHALINAE
model_glo = gam(n_individuals ~ offset(log_surface) +
                s(NASC, k = 16, bs = "cr", by = vertical_layer) +
                s(SST, k = 4, bs = "cr") +
                s(log_chloro, k = 4, bs = "cr") +
                s(d20, k = 4, bs = "cr") +
                s(bathy,k = 4, bs = "cr"),
                family= tw(link ='log'),
                method= "REML",
                data= df_GLOB)
#### ZIPHIIDAE
model_zip = gam(n_individuals ~ offset(log_surface) +
                s(NASC, k = 16, bs = "cr", by = vertical_layer) +
                s(SST, k = 4, bs = "cr") +
                s(log_chloro, k = 4, bs= "cr") +
                s(d20, k = 4, bs = "cr") +
                s(bathy,k = 4, bs = "cr"),
                family= tw(link ='log'),
                method= "REML",
                data= df_ZIPH)
#### WEDGE-TAILED SHEARWATER
model_wtsh = gamm(foraging_numeric ~ s(NASC, k = 8, bs= "cr", by = moment) +
                s(SST, k = 4, bs= "cr") +
                s(log_chloro, k = 4, bs = "cr") +
                s(d20, k = 4, bs= "cr") +
                s(bathy, k = 4, bs= "cr"),
                data = df_puffin,
                method="REML",
                correlation = corARMA(form = ~ 1 | Individu, p = 2),
                family = binomial)
#### TAHITI PETREL
model_tapet = gamm(foraging_numeric ~ s(NASC, k = 8, bs = "cr", by = moment) +
                s(SST, k = 4, bs = "cr") +
                s(log_chloro, k = 4, bs = "cr") +
                s(d20, k = 4, bs = "cr") +
                s(bathy, k = 4, bs = "cr"),
                data = df_puffin,
                method="REML",
                correlation = corARMA(form = ~ 1 | Individu, p = 2),
                family = binomial)
#### RED-FOOTED BOODY
model_rfbo = gamm(foraging_numeric ~ s(NASC, k = 8, bs = "cr", by = moment) +
                s(SST, k = 4, bs = "cr") +
                s(log_chloro, k = 4, bs = "cr") +
                s(d20, k = 4, bs = "cr") +
                s(bathy, k = 4, bs = "cr"),
                data = df_puffin,
                method="REML",
                correlation = corARMA(form = ~ 1 | Individu, p = 2),
                family = binomial)


##############################################################################
############################## Prediction ####################################
########### Fish
load(file ='df_grid_for_pred_fish.Rdata')

data.table(df_grid_for_pred_fish)
lon      lat vertical_layer date     SST     d20   chloro  NASC   bathy
```

```
156.05   -19.30   epi         2010-01-01   26.80   237.25   0.023   3.698   2.85
156.05   -19.30   epi         2010-01-08   27.30   229.75   0.023   3.697   2.85
156.05   -19.30   epi         2010-01-15   27.25   227.95   0.039   3.733   2.85
156.05   -19.30   epi         2010-01-22   28.13   235.14   0.060   3.728   2.85
156.05   -19.30   epi         2010-01-29   27.99   248.44   0.029   3.734   2.85
   ---
174.30   -25.05   uper_meso   2018-12-03   23.53   136.39   0.088   1.807   4.46
174.30   -25.05   uper_meso   2018-12-10   23.88   158.98   0.069   1.947   4.46
174.30   -25.05   uper_meso   2018-12-17   25.16   171.19   0.082   1.850   4.46
174.30   -25.05   uper_meso   2018-12-24   25.45   191.67   0.073   1.971   4.46
174.30   -25.05   uper_meso   2018-12-31   26.26   221.23   0.081   1.896   4.46
```

```r
df_grid_for_pred_fish$vessel_code <- "24080"
df_grid_for_pred_fish$n_hook      <- mean(df_ALB$n_hook)
df_grid_for_pred_fish$log_chloro <- log(df_grid_for_pred_fish$chloro + 1)
## this next table was extracted from the observed dataset (df_ALB) to have the min and the max of each variable and therefore
avoid extrapolation
df_min_max_alb
  sp    variable    max      min
1 ALB   bathy       5.9596   0.0040
2 ALB   SST         30.374   20.651
3 ALB   d20         283.39   69.162
4 ALB   log_chloro  0.4579   0.0167
5 ALB   NASC        4.1644   0.3300

df_grid_for_pred_fish$extrapolation <-ifelse(df_grid_for_pred_fish$bathy %between%
            c(df_min_max_alb[df_min_max_alb$variable == 'bathy', 'min'],
             df_min_max_alb[df_min_max_alb$variable == 'bathy', 'max']) &
                    df_grid_for_pred_fish$log_chloro %between%
            c(df_min_max_alb[df_min_max_alb$variable == 'log_chloro', 'min'],
             df_min_max_alb[df_min_max_alb$variable == 'log_chloro', 'max']) &
                    df_grid_for_pred_fish$d20 %between%
            c(df_min_max_alb[df_min_max_alb$variable == 'd20', 'min'],
             df_min_max_alb[df_min_max_alb$variable == 'd20', 'max']) &
                    df_grid_for_pred_fish$SST %between%
            c(df_min_max_alb[df_min_max_alb$variable == 'SST', 'min'],
             df_min_max_alb[df_min_max_alb$variable == 'SST', 'max'])&
                    df_grid_for_pred_fish$NASC%between%
            c(df_min_max_alb[df_min_max_alb$variable == 'NASC', 'min'],
             df_min_max_alb[df_min_max_alb$variable == 'NASC', 'max']),
                    'NO', 'YES')
df_grid_for_pred_fish <- df_grid_for_pred_fish %>%
            dplyr::filter(extrapolation == 'NO') %>%
            dplyr::select(extrapolation)

df_grid_for_pred_fish$pred_alb  <- predict(model_alb, df_grid_for_pred_fish, 'response')
df_grid_for_pred_fish$pred_alb_SE<- predict(model_alb, df_grid_for_pred_fish, 'response', se =TRUE)$se

df_grid_for_pred_fish$month<- substr(df_grid_for_pred_fish$date, 6, 7)

df_grid_for_pred_fish2 <- df_grid_for_pred_fish %>%
            group_by(month, lon, lat) %>%
            summarize(pred_nb_alb = mean(pred_nb_alb/hook),
                pred_nb_alb_se = mean(pred_nb_alb_se/hook))
```

```r
## and in the same way, predictions were for the two other fish species
########## Cetacean
load(file ='df_grid_for_pred_cetacean.Rdata')

data.table(df_grid_for_pred_cetacean)## only months 10, 11 and 12 (sampled month)
vertical_layer NASC    date        lon     lat    SST    d20     chloro  bathy
epi        1.10  2010-10-05  163.05  -14.55  26.83  262.30  0.0485  4.31
up_meso    0.32  2010-10-05  163.05  -14.55  26.83  262.30  0.0485  4.31
low_meso   2.26  2010-10-05  163.05  -14.55  26.83  262.30  0.0485  4.31
epi        1.10  2010-10-05  163.30  -14.55  26.76  261.34  0.0426  3.95
up_meso    0.32  2010-10-05  163.30  -14.55  26.76  261.34  0.0426  3.95
   ---                                              epi        1.02   2018-12-30  166.05  -26.55  23.88
82.65  0.0661  3.57
up_meso    0.35  2018-12-30  166.05  -26.55  23.88  82.65  0.0661  3.57
low_meso   1.86  2018-12-30  166.05  -26.55  23.88  82.65  0.0661  3.57
epi        1.16  2018-12-30  166.30  -26.55  23.92  79.67  0.0632  3.56
up_meso    0.27  2018-12-30  163.30  -26.55  23.92  79.67  0.0632  3.56

df_grid_for_pred_cetacean$surface<- mean(df_DELPH$surface)
df_grid_for_pred_cetacean$log_surface<- log(df_grid_for_pred_cetacean$surface)
df_grid_for_pred_cetacean$log_chloro <- log(df_grid_for_pred_cetacean$chloro + 1)
df_min_max_delph
```

```
   sp      variable     max      min
1 DELPH     bathy       4.943    0.002
2 DELPH     SST         28.67    21.53
3 DELPH     d20         277.47   44.62
4 DELPH     log_chloro  0.2220   0.039
5 DELPH     NASC        2.4965   0.218
```

```r
df_grid_for_pred_cetacean$extrapolation <-ifelse(df_grid_for_pred_cetacean$bathy %between%
          c(df_min_max_delph[df_min_max_delph$variable == 'bathy', 'min'],
            df_min_max_delph[df_min_max_delph$variable == 'bathy', 'max']) &
                    df_grid_for_pred_cetacean$log_chloro %between%
          c(df_min_max_delph[df_min_max_delph$variable == 'log_chloro', 'min'],
            df_min_max_delph[df_min_max_delph$variable == 'log_chloro', 'max']) &
                    df_grid_for_pred_cetacean$d20 %between%
          c(df_min_max_delph[df_min_max_delph$variable == 'd20', 'min'],
            df_min_max_delph[df_min_max_delph$variable == 'd20', 'max']) &
                    df_grid_for_pred_cetacean$SST %between%
          c(df_min_max_delph[df_min_max_delph$variable == 'SST', 'min'],
            df_min_max_delph[df_min_max_delph$variable == 'SST', 'max'])&
                    df_grid_for_pred_cetacean$NASC%between%
          c(df_min_max_delph[df_min_max_delph$variable == 'NASC', 'min'],
            df_min_max_delph[df_min_max_delph$variable == 'NASC', 'max']),
                    'NO', 'YES')

df_grid_for_pred_cetacean <- df_grid_for_pred_cetacean %>%
          dplyr::filter(extrapolation == 'NO') %>%
          dplyr::select(extrapolation)

df_grid_for_pred_cetacean$pred_delph <- predict(model_delph,
                    df_grid_for_pred_cetacean, 'response')
df_grid_for_pred_cetacean$pred_delph_SE <- predict(model_delph,
                    df_grid_for_pred_cetacean,
                    'response', se =TRUE)$se

df_grid_for_pred_cetacean$month<- substr(df_grid_for_pred_cetacean$date, 6, 7)

df_grid_for_pred_cetacean2 <- df_grid_for_pred_cetacean %>%
                    group_by(month, lon, lat) %>%
                    summarize(pred_delph = mean((pred_delph/surface)),
                        pred_delph_se = mean((pred_delph_SE/surface)))

########## Seabirds
load(file ='df_grid_for_pred_wtsh.Rdata')

data.table(df_grid_for_pred_wtsh) ## only months 5 and 6
moment NASC    date       lon     lat     SST     d20     bathy   chloro
Night  10.409  2010-05-07 163.05  -14.85  28.761  239.29  4.312   0.1238
Day    2.4979  2010-05-07 163.05  -14.85  28.761  239.29  4.312   0.1238
Night  10.200  2010-05-07 162.30  -14.05  28.690  236.55  4.598   0.1355
Day    2.5698  2010-05-07 162.30  -14.05  28.690  236.55  4.598   0.1355
----
Night  12.590  2018-06-29 165.85  -26.30  22.037  125.12  3.448   0.1778
Day    2.8979  2018-06-29 165.85  -26.30  22.037  125.12  3.448   0.1778
Night  12.591  2018-06-29 166.05  -26.30  22.452  132.35  3.574   0.1822
Day    2.7207  2018-06-29 166.05  -26.30  22.452  132.35  3.574   0.1822

df_grid_for_pred_wtsh$log_chloro <- log(df_grid_for_pred_wtsh$chloro + 1)
df_min_max_wtsh
   sp     variable     max      min
1 WTSH    bathy        7.034    0.0004
2 WTSH    SST          29.75    24.96
3 WTSH    d20          248.29   94.28
4 WTSH    log_chloro   0.4729   0.0293
5 WTSH    NASC         17.766   1.596

df_grid_for_pred_wtsh$extrapolation <-ifelse(df_grid_for_pred_wtsh$bathy %between%
          c(df_min_max_wtsh[df_min_max_wtsh$variable == 'bathy', 'min'],
            df_min_max_wtsh[df_min_max_wtsh$variable == 'bathy', 'max']) &
                    df_grid_for_pred_wtsh$log_chloro %between%
          c(df_min_max_wtsh[df_min_max_wtsh$variable == 'log_chloro', 'min'],
            df_min_max_wtsh[df_min_max_wtsh$variable == 'log_chloro', 'max']) &
                    df_grid_for_pred_wtsh$d20 %between%
          c(df_min_max_wtsh[df_min_max_wtsh$variable == 'd20', 'min'],
            df_min_max_wtsh[df_min_max_wtsh$variable == 'd20', 'max']) &
                    df_grid_for_pred_wtsh$SST %between%
          c(df_min_max_wtsh[df_min_max_wtsh$variable == 'SST', 'min'],
            df_min_max_wtsh[df_min_max_wtsh$variable == 'SST', 'max'])&
```

```
                          df_grid_for_pred_wtsh$NASC%between%
              c(df_min_max_wtsh[df_min_max_wtsh$variable == 'NASC', 'min'],
                df_min_max_wtsh[df_min_max_wtsh$variable == 'NASC', 'max']),
                                   'NO', 'YES')

df_grid_for_pred_wtsh <- df_grid_for_pred_wtsh %>%
                dplyr::filter(extrapolation == 'NO') %>%
                dplyr::select(extrapolation)

df_grid_for_pred_wtsh$pred_wtsh <- predict(model_wtsh, df_grid_for_pred_wtshs,
                          'response')
df_grid_for_pred_wtsh$pred_wtsh_SE <- predict(model_wtsh,
                          df_grid_for_pred_wtshs,
                          'response', se =TRUE)$se

df_grid_for_pred_wtsh$month<- substr(df_grid_for_pred_wtshs$date, 6, 7)

df_grid_for_pred_wtsh2 <- df_grid_for_pred_wtsh %>%
                group_by(month, lon, lat) %>%
                summarize(pred_wtsh= mean((pred_wtsh)),
                     pred_wtsh_se = mean((pred_wtsh_SE)))
```
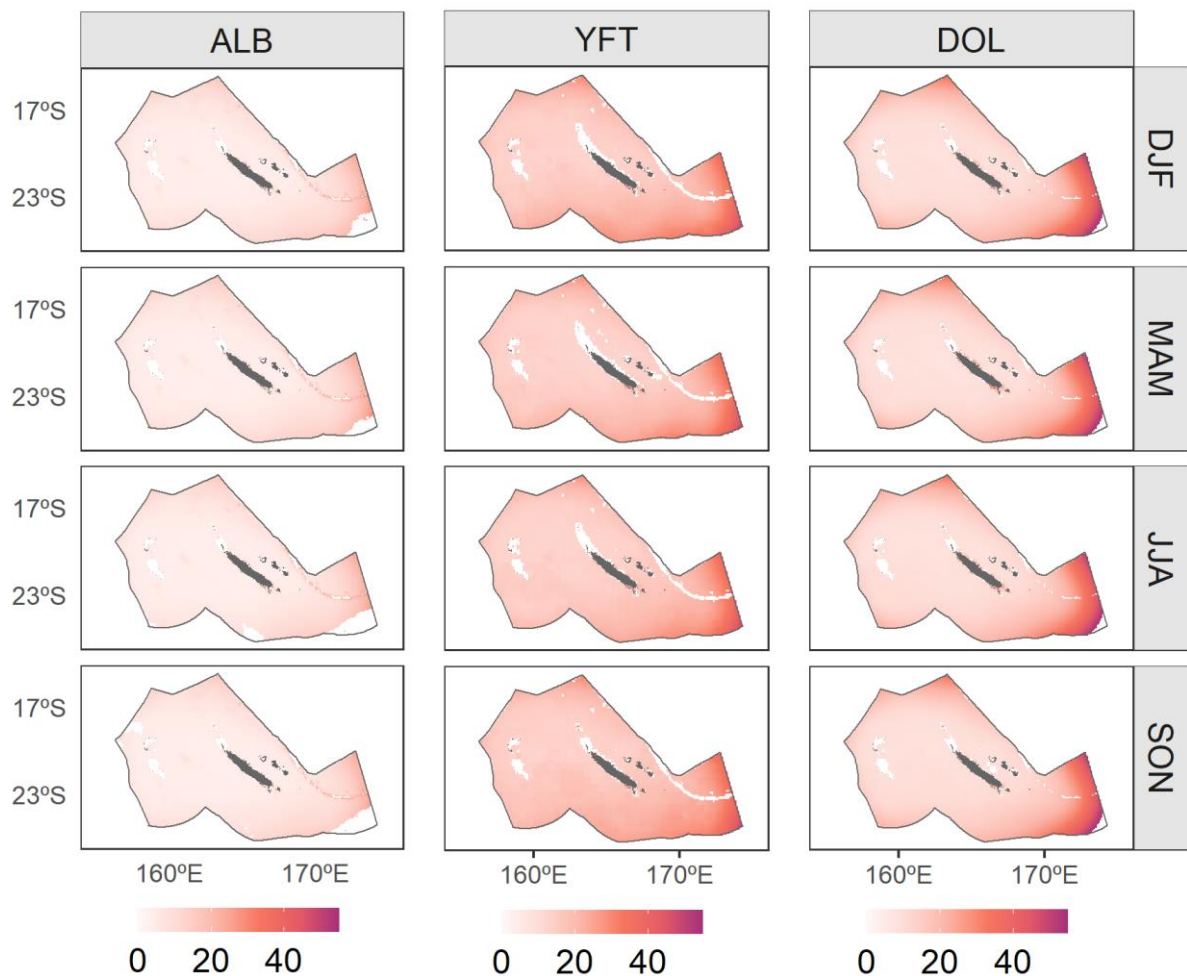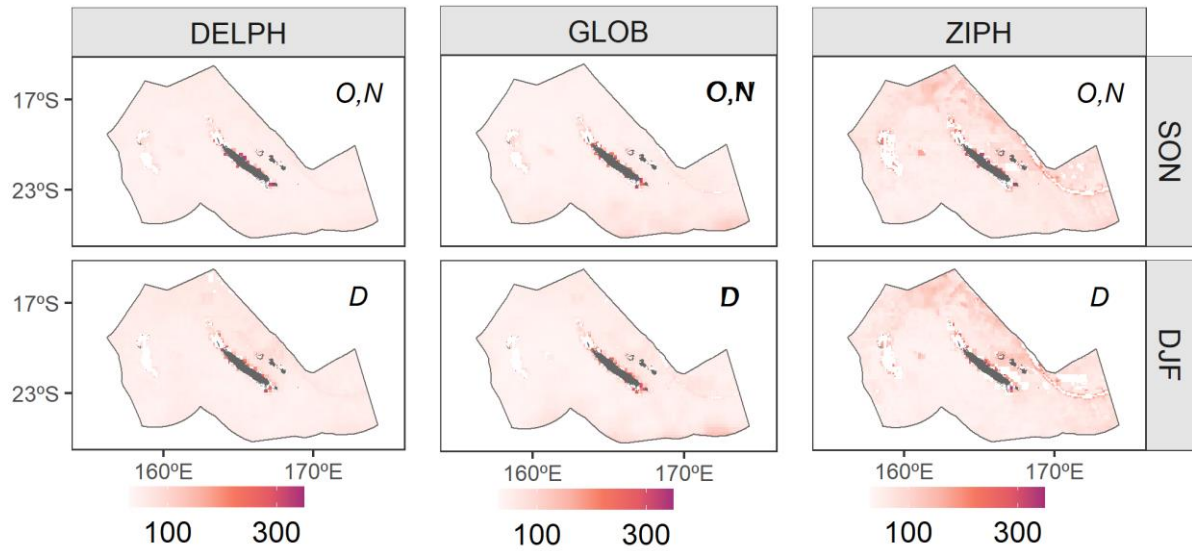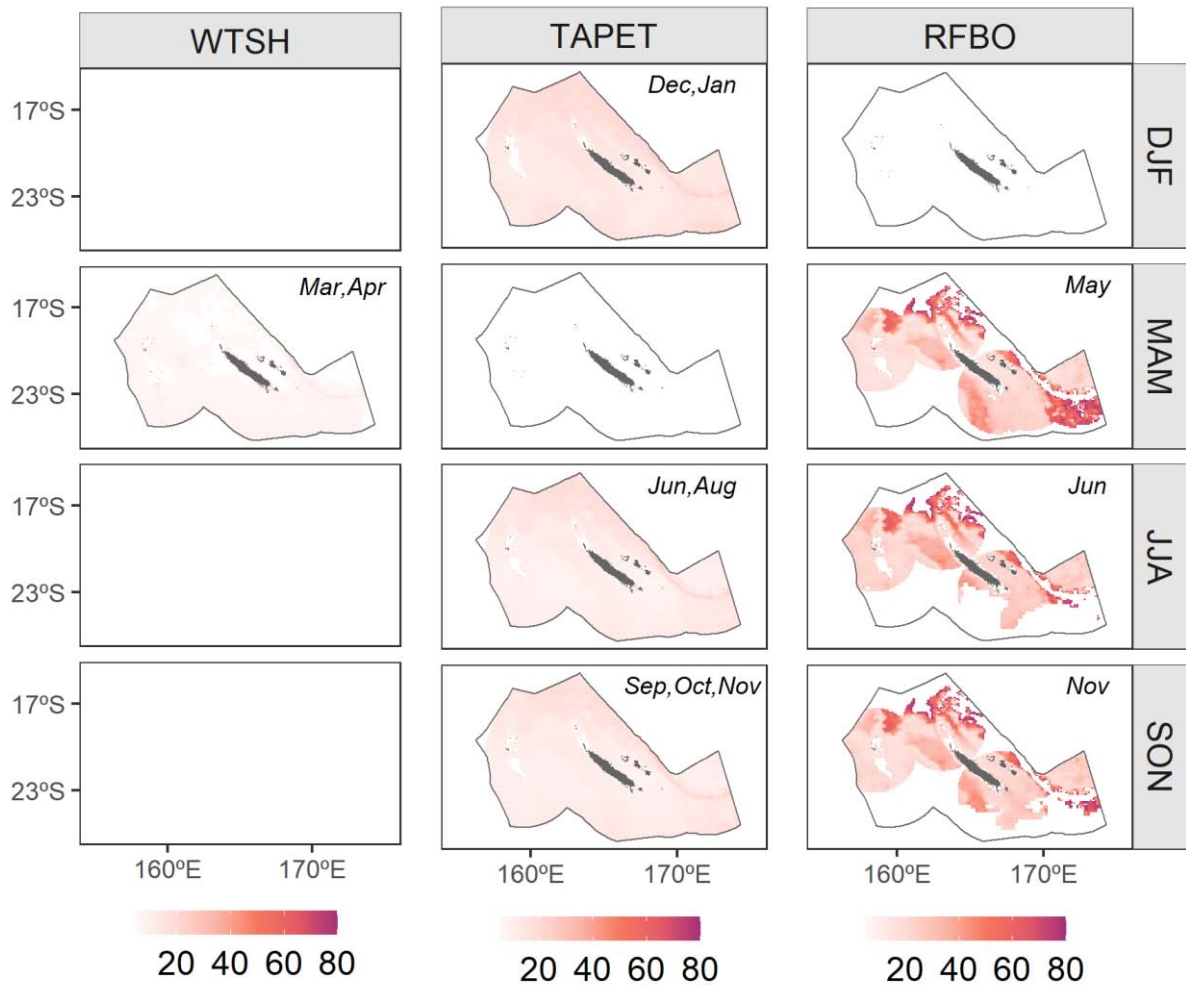
Supplementary Figure S6. Spatial predictions of standard error (expressed in %) for catch per unit of effort (CPUE; number of fish caught per 100 hooks) of albacore (ALB), yellowfin tuna (YFT) and dolphinfish (DOL), by quarter in the New Caledonian EEZ. DJF: December, January and February; MAM: March, April and May; JJA: June, July and August; SON: September, October and November. Land is represented in grey. Reef and island names are indicated on Figure 1A. Areas in white include areas where no extrapolation was made and waters with bathymetry shallower than 300 m (identified on Figure 1).

Supplementary Figure S7. Spatial predictions of standard error (expressed in %) for counts of individuals (of Delphininae (DELPH), Globicephalinae (GLOB) and Ziphiidae (ZIPH), by quarter in the New Caledonian EEZ. DJF: December, January and February; MAM: March, April and May; JJA: June, July and August; SON: September, October and November. Land is represented in grey. Reef and island names are indicated on Figure 1A. Areas in white include areas where no extrapolation was made and waters with bathymetry shallower than 300 m (identified on Figure 1).

Supplementary Figure S8. Spatial predictions of standard error (expressed in %) for foraging probability of the wedge-tailed shearwater (WTSH), the Tahiti petrel (TAPET) and the red-footed booby (RFBO), by quarter in the New Caledonian EEZ. DJF: December, January and February; MAM: March, April and May; JJA: June, July and August; SON: September, October and November. Reef and island names are indicated on Figure 1A. Areas in white include areas where no extrapolation was made and waters with bathymetry shallower than 300 m (identified on Figure 1).